Geological Quarterly, 2021, 65: 26
DOI: http://dx.doi.org/10.7306/gq.1594

Thermogenic gases generated from coals and carbonaceous shales of the Upper Silesian and Lublin Coal basins: a hydrous pyrolysis approach

Maciej J. KOTARBA[1, *], Elżbieta BILKIEWICZ[1], Krzysztof JUREK[1], Marta WALICZEK[1], Dariusz WIĘCŁAW[1] and Hieronim ZYCH[1]

[1] AGH University of Science and Technology, Faculty of Geology, Geophysics and Environmental Protection, Al. A. Mickiewicza 30, 30-059 Kraków, Poland

Kotarba, M.J., Bilkiewicz, E., Jurek, K., Waliczek, M., Więcław, D., Zych, H., 2021. Thermogenic gases generated from coals and carbonaceous shales of the Upper Silesian and Lublin Coal basins: a hydrous pyrolysis approach. Geological Quarterly, 65: 26, doi: 10.7306/gq.1594

In order to provide a better characterization of the origin and volume of thermogenic gas generation, hydrous pyrolysis (HP) experiments were performed on coals and carbonaceous shales of the Upper Silesian and Lublin Coal Basins at 330 and 360°C for 72 h. The maturity range of coals and shales used for HP varies from 0.57 to 0.92% R_o. The maturity increase caused by HP at 330 and 360°C ranges from 1.32 to 1.39% and from 1.71 to 1.83%, respectively. The ^{13}C of CH_4, C_2H_6, C_3H_6 and *n*-C_4H_{10} in gases *versus* their reciprocal C-number have a concave relationship, and therefore do not follow a linear trend. The ^{2}H of CH_4, C_2H_6 and C_3H_6 in gases *versus* their reciprocal H-number show both linear and convex-concave relationships. The growth of CO_2 yields during HP was higher for shales than for coals. H_2S yields from shales are higher than from coals, which can be associated with the catalytic and adsorbed influence of the shale matrix. H_2 was also generated in considerable quantities from water and organic matter in the coals, and in larger amounts from the shales. N_2 yields grow with an increase in R_o after 360°C HP and are more enriched in the ^{15}N isotope than after 330°C.

Key words: hydrous pyrolysis gas, gaseous hydrocarbons, carbon dioxide, molecular nitrogen, stable C, H, N isotopes, Upper Silesian Coal and Lublin Coal basins.

INTRODUCTION

In Poland, major resources of bituminous (hard) coals occurring in the Serpukhovian (Mississippian) and Pennsylvanian strata of the Upper Silesian Coal Basin (USCB) and Lublin Coal Basin (LCB; Fig. 1) belong to the Euro-American coal province. Methane is the dominant gas within bituminous coal seams in the USCB and LCB (Kotarba, 2001).

Previous studies of molecular and stable carbon and hydrogen isotope compositions of coalbed gases accumulated in the USCB and LCB (Kotarba, 1990a, 2001; Kotarba and Pluta, 2009; Kotarba et al., 2019a) revealed that in addition to thermogenic methane and carbon dioxide, and smaller quantities of higher gaseous hydrocarbons, microbial methane and carbon dioxide are also present; these gases also occur in the abandoned Lower Silesian Coal Basin (LSCB; Kotarba, 1988, 1990b, c; Kotarba and Rice, 2001; Sechman et al., 2013). At times great quantities of endogenic carbon dioxide migrated from mantle and/or magmatic bodies in lithosphere through deep-seated faults, to accumulate within the Carboniferous coal-bearing strata of the LSCB (Kotarba, 1990c; Kotarba and Rice, 2001). However, because of difficult and complicated geological, gaseous and hydrogeological conditions, all mines in the LSCB have been closed in years 1991–2001 (Sechman et al., 2013, 2017). The thermogenic gases were generated from coal seams and dispersed organic matter in shale (claystone and mudstone) successions during the coalification, a process completed at the end of the Variscan orogeny (around the Pennsylvanian/Permian boundary; Kotarba, 2001; Kotarba and Pluta, 2009). In the USCB, secondary microbial methane and insignificant amounts of carbon dioxide were generated within the Pennsylvanian coal-bearing strata as a result of infiltration of meteoric waters together with methanogenic bacteria and nutrients in the Paleogene and Early Miocene (Kotarba and Pluta, 2009). The balance of methane generation and accumulation has been evaluated by Kotarba et al. (1995a, b) and Kowalski et al. (1995).

The first qualitative and quantitative evaluation models of thermogenic gases generated during coalification based on the balance of changes in elemental composition and organic matter mass were published by Karweil (1966, 1969), Jüntgen and Karweil (1966), Jüntgen and Klein (1975), Kotarba (1988), Kowalski et al. (1995). However, this method is affected by considerable error due to the unreliability of determining mass losses during coalification (Jüntgen and Karweil, 1966; Kotarba, 1988). Laboratory techniques of hydrous pyrolysis (HP) and anhydrous pyrolysis have been effectively used for

* Corresponding author, e-mail: kotarba@agh.edu.pl

Received: December 17, 2020; accepted: April 1, 2021; first published online: June 1, 2021

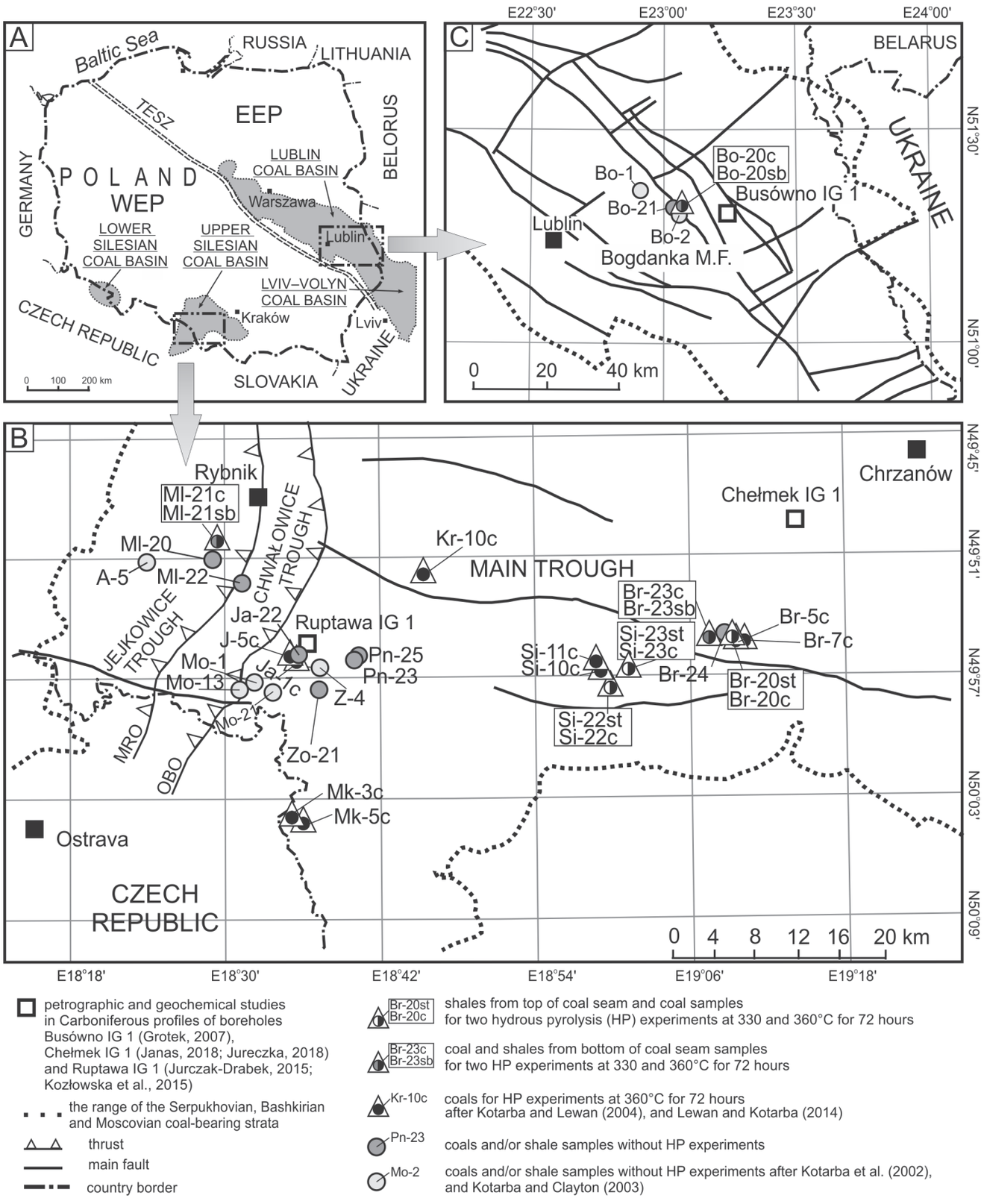

Fig. 1A – general sketch map of Poland; B – the southern part of the Upper Silesian Coal Basin and the western part of the Carpathian Foredeep; C – the Lublin Coal Basin, showing the location of rock sampling sites

WEP – West European Platform, EEP – East European Platform, TESZ – Trans-European Suture Zone, MRO – Michálkovice–Rybnik Overthrust, OBO – Orlová–Boguszowice Overthrust, M.F. – Mine Field

simulating coal maturation (e.g., Geissler and Belau, 1971; Higgs, 1986; Lu and Kaplan, 1990; Landais, 1991; Teerman and Hwang, 1991; Hill et al., 1994; Qin et al., 1994; Andresen et al., 1994, 1995; Behar et al., 1997; Kotarba and Lewan, 2004; Shuai et al., 2013; Lewan and Kotarba, 2014; Gao et al., 2020).

HP has been used for simulating natural thermal maturation of organic matter and its transformation to crude oil and natural gas (e.g., Lewan, 1985, 1993, 1997, 2002). This method best simulates natural petroleum formation because liquid water existing in the subsurface is an important source of hydrogen and a facilitator of oil expulsion (Lewan, 1997). Although HP of humic coals has been shown to generate less thermogenic gas than other, anhydrous pyrolysis method, the quantities of gas generated remain excessive as compared to gas accumulations in the Polish coal basins (Kotarba and Lewan, 2004; Lewan and Kotarba, 2014). Lewan and Kotarba (2014) have conducted HP on a global set of coals representing ranks from lignite through to bituminous coal, meta-anthracite and graphite to determine changes in their potential for gas generation and the rank limit to primary gas generation.

This paper describes the simulation, generation and evaluation of the yields of hydrocarbon (CH_4, C_2H_6, C_3H_8, *i*-C_4H_{10}, *n*-C_4H_{10}, *i*-C_5H_{12}, *n*-C_5H_{12}, C_6H_{14}, C_7H_{16} and unsaturated hydrocarbons) and non-hydrocarbon (CO_2, N_2, H_2 and H_2S) components of thermogenic gases expelled from coals and carbonaceous shales by HP experiments at 330 and 360°C for 72 hours corresponding to two steps of coalification, of 1.3–1.4% and 1.7–1.8% on the vitrinite reflectance scale, respectively. Moreover, based on the results of the HP yields, the molecular composition and stable carbon [$^{13}C(CH_4)$, $^{13}C(C_2H_6)$, $^{13}C(C_3H_8)$, $^{13}C(i\text{-}C_4H_{10})$, $^{13}C(n\text{-}C_4H_{10})$, $^{13}C(i\text{-}C_5H_{12})$, $^{13}C(n\text{-}C_5H_{12})$, $^{13}C(CO_2)$], hydrogen [$^{2}H(CH_4)$, $^{2}H(C_2H_6)$, $^{2}H(C_3H_8)$] and nitrogen [$^{15}N(N_2)$] isotope analyses of the expelled HP gases, and the genetic relations of hydrocarbons, carbon dioxide, molecular nitrogen and hydrogen sulphide are explained. Interpretation of the results of the HP experiments and analyses was made in relation to the genetic type of source organic matter (Rock-Eval data, and elemental composition and atomic H/S, O/C, N/C and S_{org}/C ratios) and maturity rank (Rock-Eval T_{max}, R_o, VM^{daf}, H/C_{at}). The results of previously published HP experiments at 360°C for 72 hours and geochemical studies of coals (Kotarba et al., 2002; Kotarba and Clayton, 2003; Kotarba and Lewan, 2004; Lewan and Kotarba, 2014) from the USCB and LCB and other basins are also used for genetic interpretation.

GEOLOGICAL SETTING

UPPER SILESIAN COAL BASIN

The USCB, one of the major coal basins in the world, formed as a foredeep of the Moravo-Silesian fold belt. It is a deep molasse basin of polygenetic origin: the lower part of the Upper Mississippian (Serpukhovian) coal-bearing lithostratigraphic succession reflects a paralic depositional system, while the Pennsylvanian coal-bearing lithostratigraphic succession (Bashkirian and Moscovian) is of continental origin (Fig. 2). The Upper Silesian Variscan orogen formed in several phases. Uplift and compression producing the main fold structures, such as the Jejkowice, Chwałowice and Main troughs (Fig. 1), took place during the Asturian and Leonian orogenic phases in end-Pennsylvanian and early Permian times (Kotas, 1982, 1994; Kotas et al., 1983; Kotas and Porzycki, 1984; Buła and Kotas, 1994; Buła and Żaba, 2005; Jureczka et al., 2005; Kędzior et al., 2007; Narkiewicz, 2007; Ćmiel, 2012 and references therein). After the Variscan uplift, the Serpukhovian and Pennsylvanian coal-bearing strata were exposed across most of the basin, and subjected to erosion and denudation. The strongest tectonic involvement has been observed among Carboniferous coal-bearing strata in the western part of the USCB, where folds and thrusts of the Moravian-Silesian belt formed. The eastern limit of these structures is determined by the Orlová–Boguszowice Overthrust in the USCB area (Fig. 1). Pennsylvanian strata in the N and NE parts of the USCB also underwent intense fold and block tectonic deformation. The origin of these structures, generally referred to as the Main Saddle (Kotas, 1982), may be associated with strike-slip stresses, an intense expression of which is observed in the nearby Kraków–Lubliniec Fault Zone dating to the Pennsylvanian/Permian boundary (Żaba, 1999). The central, eastern and western parts of the USCB are characterized by horizontal deposition of Carboniferous strata and fault tectonics that relate to processes in the Precambrian basement of Brunovistulicum (Kotas, 1982; Buła and Żaba, 2005). Structures generated in these parts of the USCB are referred to as the Main Trough (Kotas, 1982). In the southern part of the USCB (Fig. 1), the autochthonous Miocene (Karpatian–Badenian) marine, clayey-sandstone strata of the western part of the Carpathian Foredeep were deposited and overlie the Carboniferous coal-bearing strata (Peryt et al., 2005). The eroded top of the Carboniferous strata includes occasional depressions, as well as gorges and canyons >1100 m deep. At the end of the Miocene, the Outer Carpathian nappes thrusted over the autochthonous strata of the Carpathian Foredeep from the south (Oszczypko et al., 2006). During the Alpine movements, the Upper Silesian Variscan orogen behaved like a consolidated basement for the Alpides.

LUBLIN COAL BASIN

The LCB is an epi-platform, molasse basin, developed as a pericratonic depression in the transitional zone of two great geological units (i.e., the pre-Vendian Platform and Central European Paleozoic Platform) from the Upper Visean to the Moscovian (Kotas and Porzycki, 1984; Porzycki and Zdanowski, 1995a, b; Tomaszczyk and Jarosiński, 2017; Krzywiec et al., 2017; Kufrasa et al., 2019). Its Mississippian and Pennsylvanian coal-bearing lithostratigraphic succession is of polygenetic origin: the lower part (Upper Visean and Serpukhovian) is marine-paralic, the middle part (Bashkirian) is paralic, and the upper part (Moscovian) is continental (limnic-fluvial) (e.g., Porzycki, 1988a, b; Porzycki and Zdanowski, 1995a; Waksmundzka, 1998, 2010, 2013; Zdanowski, 1999, 2007; Narkiewicz, 2007, 2020; Kozłowska and Waksmundzka, 2020). The total thickness of these lithostratigraphic units changes from tens of metres in the NE to over 2000 m in the SW. Coal seams <0.5 m in thickness occur in the Mississippian (Visean and Serpukhovian) strata, associated with palaeosols and overlain by limestone beds, forming good correlation horizons. Between the Mississippian and Pennsylvanian a stratigraphic gap is documented. Pennsylvanian coal seams of economic thicknesses (>0.6 m) occur in the Lower Bashkirian and Lower Moscovian strata. Lower Bashkirian coals are exploited in the Volynian-Lviv Coal Basin in Ukraine, and Lower Moscovian coals in the LW “Bogdanka” coal mine in the central part of the LCB. After the Variscan uplift the Mississippian and Pennsylvanian coal-bearing formations were also exposed and subjected to erosion and denudation. The overburden above Carboniferous strata in the LCB is formed by the Permian (20–70 m) and Triassic (20–60 m) only in Łuków area, Jurassic (0 to >300 m), Cretaceous (300–1000 m), Tertiary (several metres) strata and Quaternary

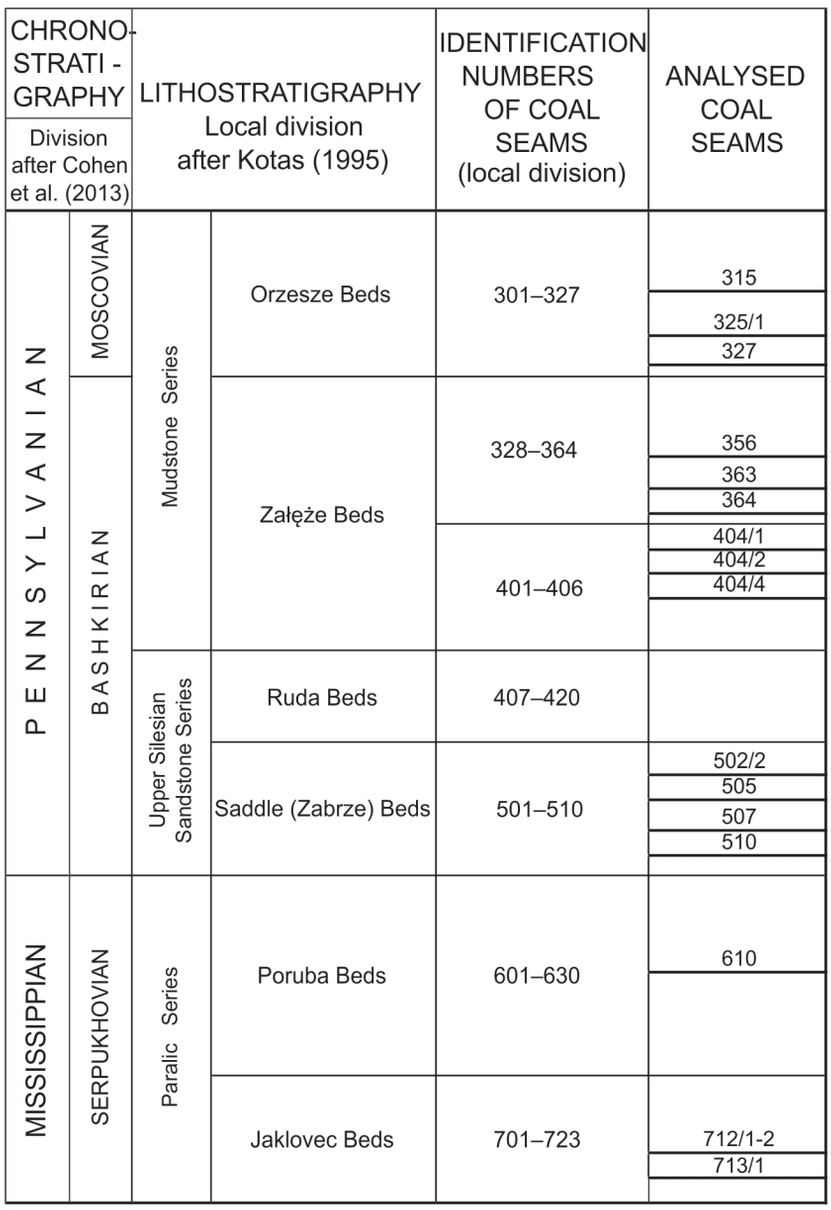

Fig. 2. Section through Mississippian and Pennsylvanian coal-bearing strata and location of coal seams in which the coals and shales analysed were collected above and below these coal seams in the study area of the Upper Silesian Coal Basin

(<100 m) sediments. Overburden thickness varies from ~350 m at the Polish-Ukrainian border to >1200 m west of Lublin (Zdanowski, 1999).

The coalification and gas generation processes both in the LCB and USCB were completed at the end of the Variscan orogeny and were not subsequently rejuvenated.

MATERIALS

Serpukhovian, Bashkirian and Moscovian 29 channel coal samples (c), and 57 block carbonaceous shale samples, the shales being collected above (st) and below (sb) coal seams in mine workings, were collected from six methane mines ("Brzeszcze", "Jastrzębie", "Marcel", "Pniówek", "Silesia" and "Zofiówka") in the USCB and one (LW "Bogdanka" mine in the LCB (Appendix 1* and Fig. 1). The locations of all current and previously studied samples from the USCB and LCB are shown in Figure 1.

After Rock-Eval II pyrolysis and vitrinite reflectance (R_o) studies (Appendix 2), we selected and prepared 6 coal samples (five from the USCB and one from the LCB) and 6 carbonaceous shale samples (five from the USCB and one from the LCB) for hydrous pyrolysis experiments and pyrolysis completed using Rock-Eval 6 apparatus: Br-20c, Br-20st, Br-23c, Br-23sb, Ml-21c, Ml-21sb, Si-22c, Si-22st, Si-23c, Si-23st, Bo-20c and Bo-20sb (Appendix 3).

* Supplementary data associated with this article can be found, in the online version, at doi: 10.7306/gq.1594

EXPERIMENTAL AND ANALYTICAL METHODS

EXPERIMENTAL HYDROUS PYROLYSIS APPROACH

HP experiments are conducted in Hastelloy C-276 1-litre reactors (Parr Instrument Co.). Rock samples placed in reactors are heated isothermally in electric heaters at 330 ±0.5°C and 360 ±0.4°C for 72.08 ±0.04 hours in the presence of liquid water. The water-to-rock proportion is based on calculations using steam tables and measured bulk rock densities to ensure that the rock samples remain in contact with liquid water throughout the experiments (Lewan, 1993). The bituminous coals and carbonaceous shales were crushed to gravel size (0.5–2.0 cm) with no prior extraction or drying before experiments. In each experiment, 300 g of crushed bituminous coal or 500 g of shale were loaded into the reactor. The reactor was closed and evacuated for several minutes before 350 g (for coals) or 380 g (for shales) of distilled water was injected into the reactor. Detailed descriptions of experimental procedure are published by Lewan (1985, 1993, 1997), Kotarba and Lewan (2004) and Lewan and Kotarba (2014).

ANALYTICAL APPROACH

The 86 original coal and carbonaceous shale samples were homogenized and pulverized to <0.2 mm. A preliminary assessment of geochemical parameters, indices and hydrocarbon potential of rock samples was determined by Delsi Rock-Eval II (R-E II) and Vinci Technologies Rock-Eval 6 (R-E 6) with *Bulk* rock method – *Basic* cycle pyrolysis apparatuses. Details of the analysis are given by Espitalié et al. (1985) and Zielińska et al. (2020).

Proximate analyses of volatile matter content (VM^{daf}) for dry-and-ash-free (daf) basis as well as moisture and ash contents in coals were conducted according to the procedures recommended by International Standards (ISO, 2010a, b, c).

Kerogen for stable carbon isotope analysis was obtained by treating solvent-extracted coals with boiling 10% hydrochloric acid for 30 minutes to remove carbonate minerals. Bitumen was extracted from pulverized aliquots of each sample in a Soxhlet apparatus with chloroform for 24 hours. Copper foil was placed in the boiling flask to remove elemental sulphur extracted from the samples. The resulting solution was filtered and the bitumen concentrated by evaporation.

Petrological analysis was carried out on polished rock samples under oil immersion using a Carl Zeiss Axio Imager A1m microscope equipped with a 50X oil immersion lens, integrated with a J&M GmbH MSP 200 photometer for reflectance measurements. Vitrinite reflectance (R_o, %) was determined by counting from 105 to 150 points per coal sample, and from 40 to 103 points per carbonaceous shale sample. The measurements of random R_o were run in accordance with the American Society for Testing and Materials guidelines (ASTM, 2005, 2011). The elemental analysis (C, H, N and S_{total}) of kerogen separated from the coals and shales was determined on a Carlo Erba 1108 elemental analyser using sulphanilamide as a standard. The sulphur contents reported refer to organic sulphur (S_{org}), which is determined by the difference between total sulphur and pyrite sulphur (Durand and Monin, 1980). The quantity of pyrite sulphur in the coals was analysed as iron, on a Perkin-Elmer Plasma 40 ICP-AES instrument after digesting the ash from the burnt coals (815°C) for 30 minutes with 20% hydrochloric acid. The oxygen content was calculated as the difference to 100% taking into account C, H, N, S_{total}, moisture, and ash contents.

The molecular composition of the HP gases (CH_4, C_2H_6, C_3H_8, *i*-C_4H_{10}, *n*-C_4H_{10}, *i*-C_5H_{12}, *n*-C_5H_{12}, C_6H_{14}, C_7H_{16}, CO_2, O_2, H_2, N_2, He) was analysed in a set of columns on two Agilent 7890A GCs equipped with a gas sampling valve plumbed with a dual sample loop. Stable carbon and nitrogen isotope analyses were performed using a *Finnigan™ Delta Plus MS* coupled through a GC combustion III interface with a HP 6890 GC. Stable hydrogen isotope analyses of methane, ethane and propane were performed in a *Thermo Scientific™ Delta V™ Plus MS* connected through *GC Isolink*™ and *Conflo IV* interfaces with a Trace GC Ultra chromatograph. The stable carbon, hydrogen and nitrogen isotope data are expressed in -notations (^{13}C, ^{2}H and ^{15}N, ‰) relative to VPDB, VSMOW and atmospheric nitrogen, respectively (Coplen, 2011). Detailed descriptions of analytical measurements of molecular and stable isotope compositions are published by Kotarba et al. (2019a, b, 2020a, b).

RESULTS

ORIGINAL COALS AND CARBONACEOUS SHALES

The results of analyses of the tested original (unheated) coals and carbonaceous shales to evaluate thermal maturity using T_{max} temperature (Rock-Eval pyrolysis), vitrinite reflectance (R_o), carbon content (C^{daf}), atomic H/C ratios and volatile matter content (VM^{daf}) are given in Appendices 2 and 4. The Rock-Eval T_{max} temperature of the coals analysed varies from 430 to 486°C and of the carbonaceous shales from 429 to 491°C (Appendix 2 and Fig. 3A, C). The R_o for coals varies from 0.60 to 1.57% and for carbonaceous shales ranges from 0.57 to 0.92% (Appendix 2 and Fig. 4).

Based on these results of T_{max} and R_o analyses, 6 coal and 6 carbonaceous shale samples (five from the USCB and one from the LCB) characterized by relatively low values of these indices (R-E II T_{max} 434 to 448°C and 435 to 443°C, R-E 6 T_{max} 421 to 435°C and 433 to 455°C, respectively; and R_o 0.60 to 0.90% and 0.57 to 0.92%, respectively; Appendices 2 and 3, Fig. 4) were selected for HP experiments. Values of C^{daf} content and atomic H/C ratios varied for the coals from 76.7 to 82.0 wt.% and 0.67 to 0.79, respectively; and for the carbonaceous shales from 73.9 to 80.6 wt.% and 0.47 to 0.70, respectively (Appendix 4 and Fig. 4A, A', B, B'). VM^{daf} of the original coals varies from 27.8 to 33.3 wt.% (Appendix 4 and Fig. 4D).

COALS AND CARBONACEOUS SHALES AFTER HP EXPERIMENTS AND HP GASES

The results of rank characteristics of the coals analysed after the HP experiments at 330 and 360°C for 72 hours are given in Appendices 3 and 4, and in Figure 4. Thermal maturity indices and parameters for the coals analysed varied for HP temperatures of 330 and 360°C as follows: T_{max} 454 to 504°C and 520 to 559°C, R_o 1.34 to 1.39% and 1.71 to 1.83%, VM^{daf} 20.3 to 22.9 wt.% and 13.9 to 19.5 wt.%, C^{daf} 81.1 to 84.7 wt.% and 83.9 to 85.8 wt.% and atomic H/C 0.55 to 0.60 and 0.47 to 0.52; and for the carbonaceous shales: T_{max} 450 to 539°C and 544 to 564°C, R_o 1.32 to 1.37 % and 1.71 to 1.74 %, C^{daf} 79.8 to 82.8 wt.% and 79.4 to 84.9 wt.% and atomic H/C 0.41 to 0.55 and 0.40 to 0.50, respectively.

The molecular composition of the HP gases expelled from the coals and carbonaceous shales is given in Appendix 5, and stable isotopic ratios ^{13}C(CH_4, C_2H_6, C_3H_8, *i*-C_4H_{10}, *n*-C_4H_{10}, *i*-C_5H_{12}, *n*-C_5H_{12} and CO_2), ^{2}H(CH_4, C_2H_6 and C_3H_8) and nitro-

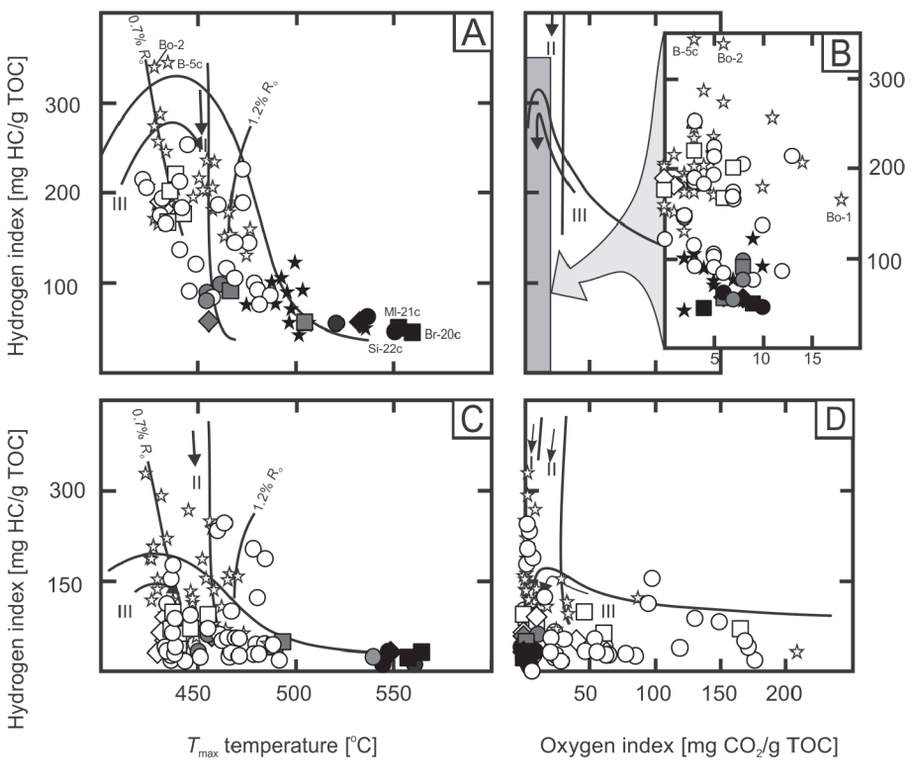

Fig. 3. Values of Rock-Eval hydrogen index *versus* (A and C) T_{max} and (B and D) oxygen index for coals (A and B) and for carbonaceous shales (C and D) of the original samples and after HP experiments at 330 and 360°C

Trend curves for different kerogen types after Espitalié et al. (1985); Rock-Eval data of current analyses are in Appendices 2 and 3, and (A and B) previously published data of the original coals (open stars) and coals after HP experiments at 360°C (filled stars) are in Kotarba and Lewan (2004) and Lewan and Kotarba (2014), and (C and D) original carbonaceous shales (open stars) in Kotarba et al. (2002); for key to stratigraphy of currently analysed samples and type of HP experiment see Figure 4

gen $^{15}N(N_2)$ are shown in Appendix 6. C_{HC} values for gases from the experiments conducted at 330°C on the coals and shales varied in the following ranges: from 3.59 to 5.08 and from 2.99 to 4.59, respectively; and at 360°C: from 4.25 to 6.07 and from 3.69 to 4.98, respectively (Appendix 6; Figs. 5A', B', C' and 6A).

During the HP experiments conducted at 330°C, methane was expelled in significant yields from the coals and carbonaceous shales and the values obtained ranged from 3.28 to 5.80 mg/g TOC_o and 1.27 to 10.0 mg/g TOC_o, respectively, and at 360°C from 8.47 to 14.0 mg/g TOC_o and 2.55 to 19.9 mg/g TOC_o, respectively (Appendix 8, Figs. 7A, B, 8 and 9A–F). The yields of ethane expelled from the coals and carbonaceous shales during the 72 hours HP experiments at 330°C were large and ranged from 0.78 to 1.54 mg/g TOC_o and 0.33 to 3.83 mg/g TOC_o, respectively, and at 360°C from 2.20 to 3.42 mg/g TOC_o and 0.64 to 6.11 mg/g TOC_o, respectively (Appendix 8, Figs. 8 and 9A'–F'). Notable amounts of propane and *n*-butane were also expelled in the course of the HP experiments (Fig. 10). The yields and concentrations of the sum of higher hydrocarbon ($(C_2\text{-}C_4)$ gases generated from the coals and shales during the 330°C HP experiments were considerable and ranged from 1.80 to 3.51 mg/g TOC_o (9.96 to 12.6 mole %) and 0.85 to 10.4 mg/g TOC_o (0.62 to 7.77 mole %), respectively, and at 360°C from 4.60 to 6.93 mg/g TOC_o (11.8 to 14.0 mole %) and 1.49 to 15.6 mg/g TOC_o (1.15 to 9.84 mole %), respectively (Appendices 5 and 8, Fig. 7C, D).

^{13}C values of methane expelled from the coals and carbonaceous shales at 330°C varied from –37.9 to –35.3‰ and –39.2 to –34.8‰, respectively, and at 360°C from –37.4 to –35.5‰ and –38.7 to –35.3‰, respectively (Appendix 6, Figs. 11, 12A, A' and 13), and ^{13}C values of ethane expelled from the coals and carbonaceous shales at 330°C varied from –28.4 to –27.4‰ and –31.4 to –28.2‰, respectively, and at 360°C from –27.4 to –26.1‰ and from –30.7 to –27.1‰, respectively (Appendix 6, Figs. 11, 12B, B' and 13). ^{13}C values of propane and *n*-butane expelled from the coals and carbonaceous shales at 330 and 360°C are shown in Appendix 6 and Figures 11, 12C, C', D, D' and 13.

^{2}H values of methane, ethane and propane expelled from the coals at 330°C varied from –313 to –270‰, –261 to –219‰, and –238 to –182‰, respectively, and at 360°C from –308 to –290‰, –252 to –225‰ and –228 to –178‰, respectively (Appendix 6, Figs. 6B and 14A, C). ^{2}H values of methane, ethane and propane expelled from the shales at 360°C for 72 hours varied from –327 to –305‰, –271 to –244‰, and –251 to –217‰, respectively, and at 360°C for 72 hours from –316 to –307‰, –268 to –244‰ and –244 to –218‰, respectively (Appendix 6, Fig. 14B, D).

During our HP experiments, carbon dioxide was generated in significant quantities from the coals and particularly from the shales during the HP experiments at 330°C ranging from 5.0 to 18.4 mg/g TOC_o and from 5.1 to 526 mg/g TOC_o, respectively (Appendix 8, Figs. 15A and 16C), and at 360°C these varied

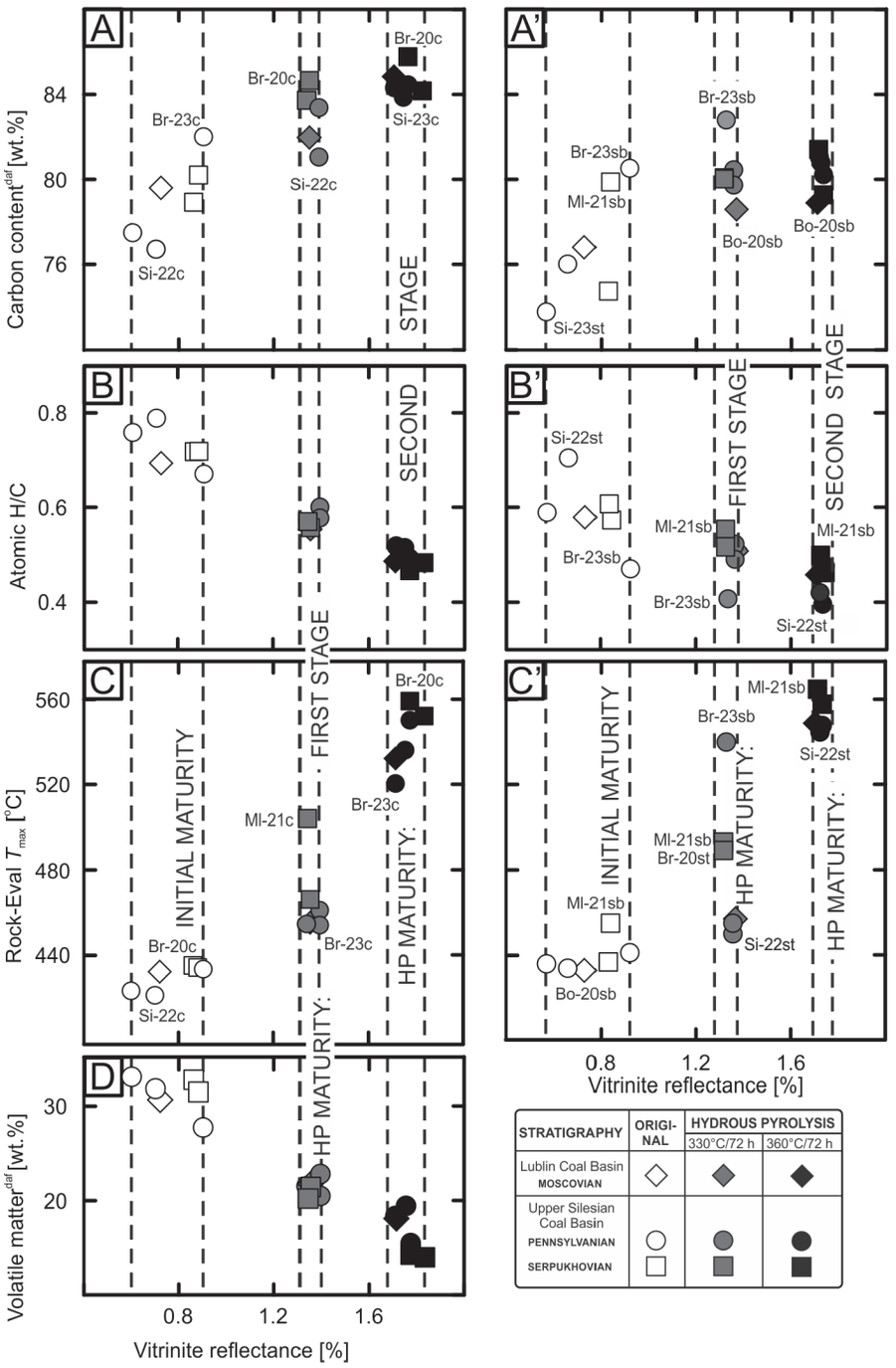

Fig. 4A – carbon content, B – atomic H/C ratio, C – Rock-Eval T_{max} temperature, D – volatile matter of the coals, A' – carbon content, B' – atomic H/C ratio, C' – Rock-Eval T_{max} temperature of the carbonaceous shales *versus* vitrinite reflectance of the original samples (INITIAL MATURITY) and samples after HP experiments at 330°C (HP MATURITY: 1st STAGE) and 360°C (HP MATURITY: 2nd STAGE)

daf – dry and ash free

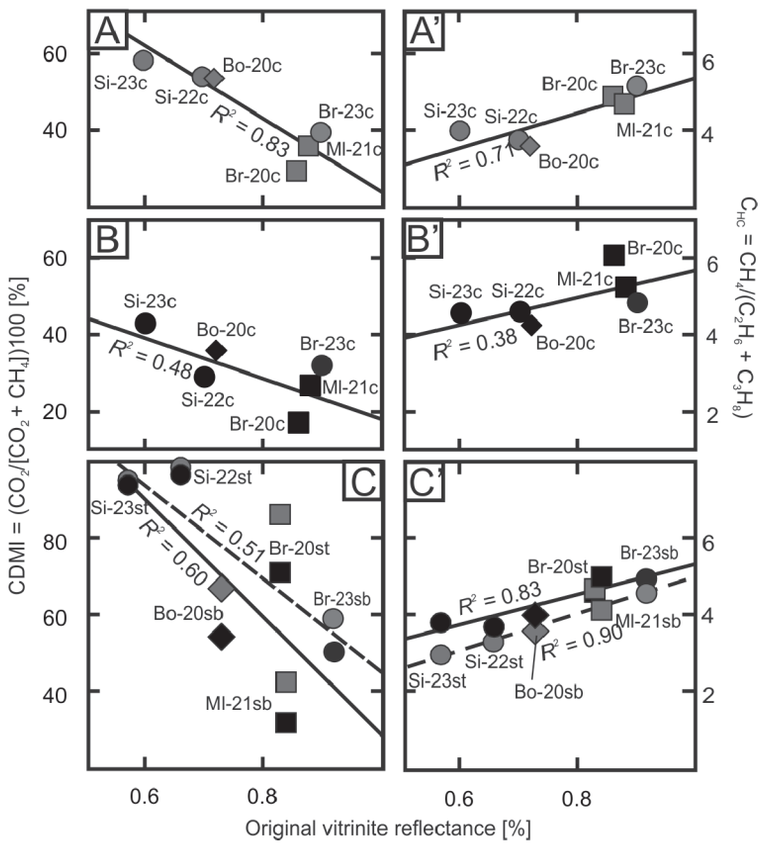

Fig. 5A–C – values of carbon dioxide-methane index (CDMI), A'–C' – hydrocarbon index (CHC) *versus* original vitrinite reflectance and for analysed HP gases generated from (A and A') coals at 330°C and (B and B') coals at 360°C, and (C and C') carbonaceous shales at 330 and 360°C

For key to stratigraphy of currently analysed samples and type of HP experiment see Figure 4

from 7.9 to 18.9 mg/g TOC_o and from 7.2 to 817 mg/g TOC_o, respectively (Appendix 8, Figs. 15A, 16C and 17A). CDMI values for gases from the HP experiments conducted at 330°C using the coals and carbonaceous shales varied in the following ranges: 29.4 to 58.5% and 42.6 to 98.3%, respectively; and at 360°C 17.1 to 42.9% and 32.1 to 96.4% (Appendix 6, Fig. 5A–C). ^{13}C values of carbon dioxide expelled from the coals and shales at 330°C varied from –21.8 to –17.0‰ and –22.6 to 3.1‰, respectively, and at 360°C from –21.7 to –17.8‰ and –23.2 to 3.7‰ (Appendix 6, Figs. 16A and 18).

Hydrogen sulphide was also generated in significant quantities and concentrations from the coals and shales during the HP experiments at 330°C, from 0.03 to 0.58 mg/g TOC_o and 0.06 to 0.99 mg/g TOC_o, respectively, and at 360°C from 0.11 to 1.06 mg/g TOC_o (0.34 to 2.43 mole %) and 0.11 to 1.16 mg/g TOC_o (0.01 to 1.98 mole %), respectively (Appendices 5 and 8, Figs. 15B, 16E and 17B).

Molecular hydrogen was also generated in notable quantities from the coals and in considerable amounts from the carbonaceous shales during the HP experiments at 330°C, from 0.04 to 0.06 mg/g TOC_o and from 0.46 to 0.99 mg/g TOC_o, respectively, and at 360°C from 0.04 to 0.06 mg/g TOC_o and from 0.53 to 3.53 mg/g TOC_o, respectively (Appendix 8, Figs. 15C, 16F and 17D).

Molecular nitrogen was expelled in significant quantities from the coals and shales during the HP experiments at 330°C, from 0.17 to 0.41 mg/g TOC_o and from 0.63 to 3.48 mg/g TOC_o, respectively, and at 360°C from 0.14 to 0.41 mg/g TOC_o and from 0.57 to 4.52 mg/g TOC_o, respectively (Appendix 8, Figs. 15D, 16D and 17C). ^{15}N values of molecular nitrogen expelled from the coals and carbonaceous shales at 330°C varied from –3.4 to 0.9‰ and from –5.6 to –0.4‰, respectively, and at 360°C from –1.3 to 0.1‰ and – from 4.3 to 1.7‰ (Appendix 6, Figs. 16B and 19).

DISCUSSION

COALS AND CARBONACEOUS SHALES BEFORE AND AFTER HP

The Serpukhovian, Bashkirian and Moskovian organic matter analysed from the LCB and southern part of the USCB (Appendix 1 and Fig. 1), accumulated within coal seams and dispersed in the carbonaceous shales, is of humic origin (type-III kerogen) and was deposited in a continental environment (Appendix 2 and Fig. 3). The maturity range of the six samples of coal and six samples of carbonaceous shale selected for the HP experiments measured by R_o varies from 0.57 to 0.92%

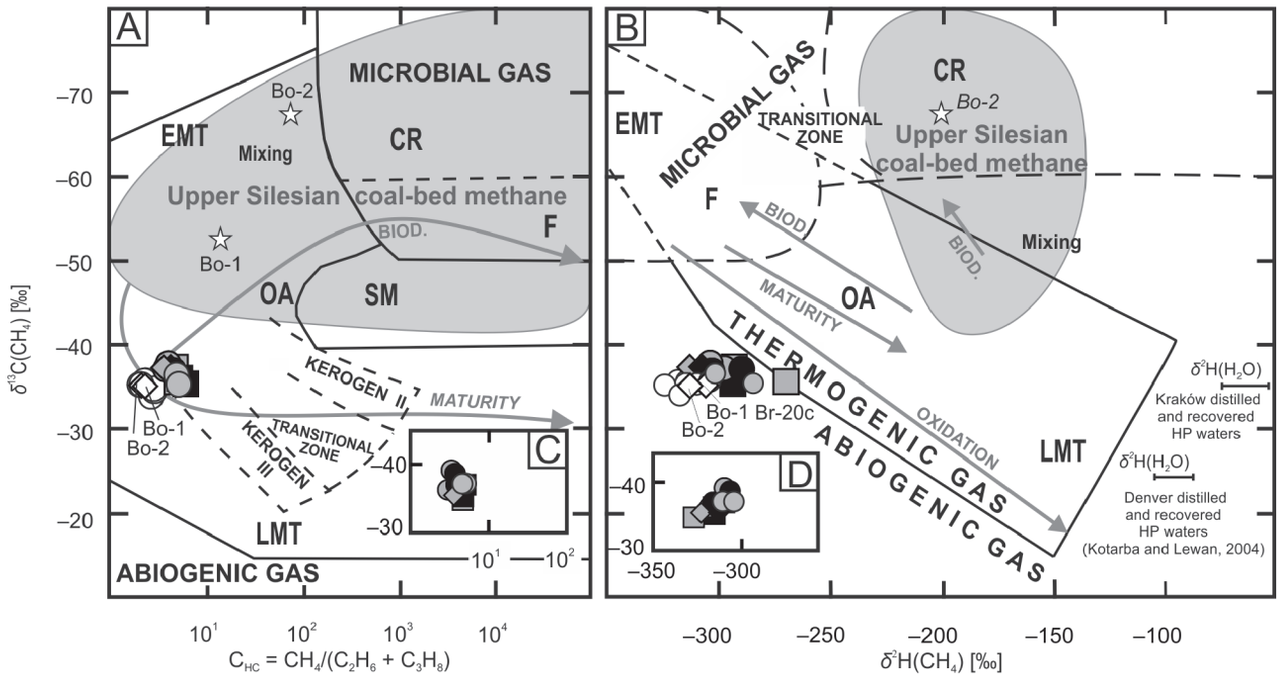

Fig. 6. Stable carbon isotope composition of methane generated during the HP experiments (330 and 360°C) *versus* values of (A and C) hydrocarbon index (CHC) and *versus* (B and D) the stable hydrogen isotope composition of CH_4

Diagrams (A) and (B) show the results for the coals and diagrams (C) and (D) the results for the carbonaceous shales; genetic fields and arrow directions of maturity and secondary processes after Whiticar (1994) and Milkov and Etiope (2018); for comparison, Upper Silesian (shaded fields) and Lublin (Bo-1 and Bo-2 open stars) coalbed methane after Kotarba (2001) and Kotarba and Pluta (2009), and Upper Silesian and Lublin (Bo-1 and Bo-2) HP gases from coals after Kotarba and Lewan (2004) and Lewan and Kotarba (2014) are also shown; for key to stratigraphy and type of HP experiment of current and previously published samples see Figure 19; CR – CO_2 reduction, F – methyl-type fermentation, SM – secondary microbial, EMT – early mature thermogenic gas, OA – oil-associated thermogenic gas; LMT – late mature thermogenic gas; BIOD. – biodegradation

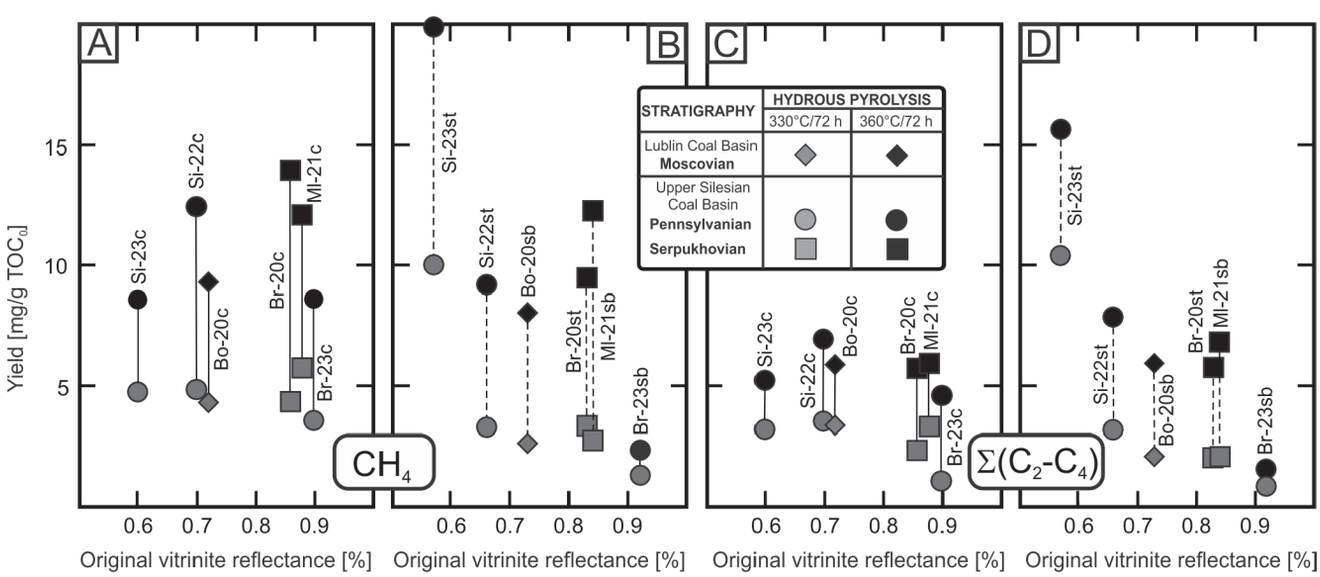

Fig. 7. Yields of methane (A and B) and sum of ethane to butanes [(C2-C4)] generated by the HP experiments at 330 and 360°C from coals (A and C) and carbonaceous shales (B and D) *versus* original vitrinite reflectance

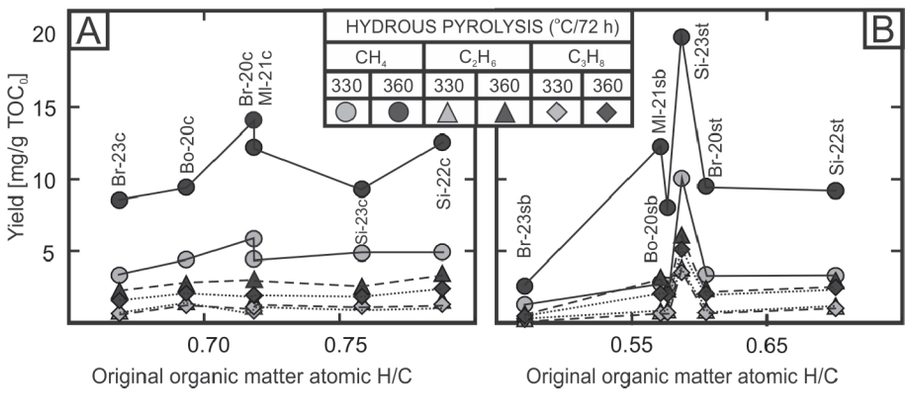

Fig. 8. Yields of methane, ethane and propane generated from original coals (A) and carbonaceous shales (B) by HP at 330 and 360°C *versus* the atomic H/C ratios of their original organic matter

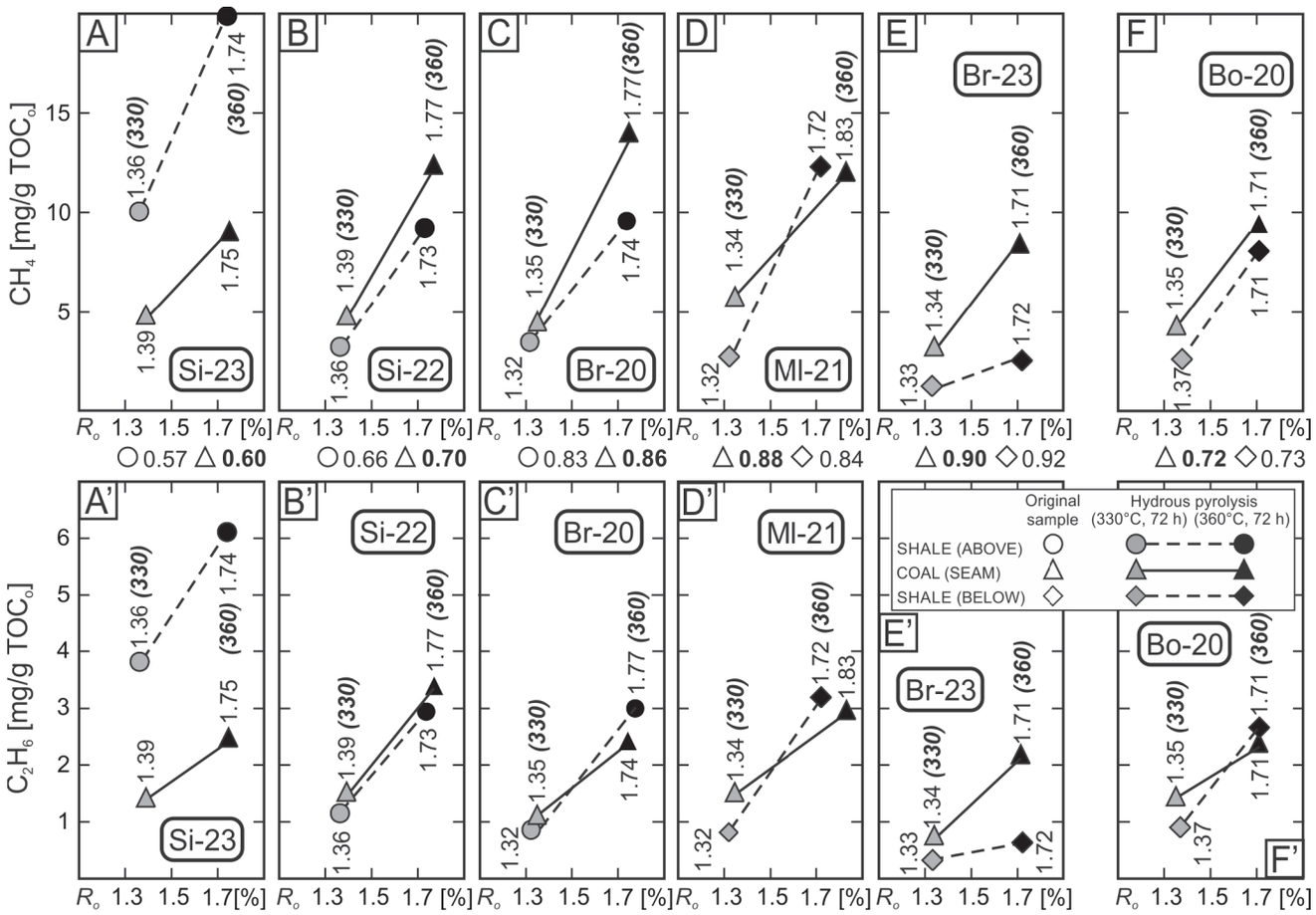

Fig. 9. Yields of (A to F in upper row) methane and (A' to F' in lower row) ethane generated from coals and carbonaceous shales of Si-23 (A and A'), Si-22 (B and B'), Br-20 (C and C'), MI-21 (D and D') and Br-23 (E and E') samples from the Upper Silesian Coal Basin, and Bo-20 sample from the Lublin Coal Basin (F and F') *versus* vitrinite reflectance after HP experiments at 330 and 360°C

Vitrinite reflectance values for original coal (triangle, bold) and carbonaceous shale (circle or rhomb, normal) are between the upper and lower rows; TOC_o – total organic carbon of original organic matter

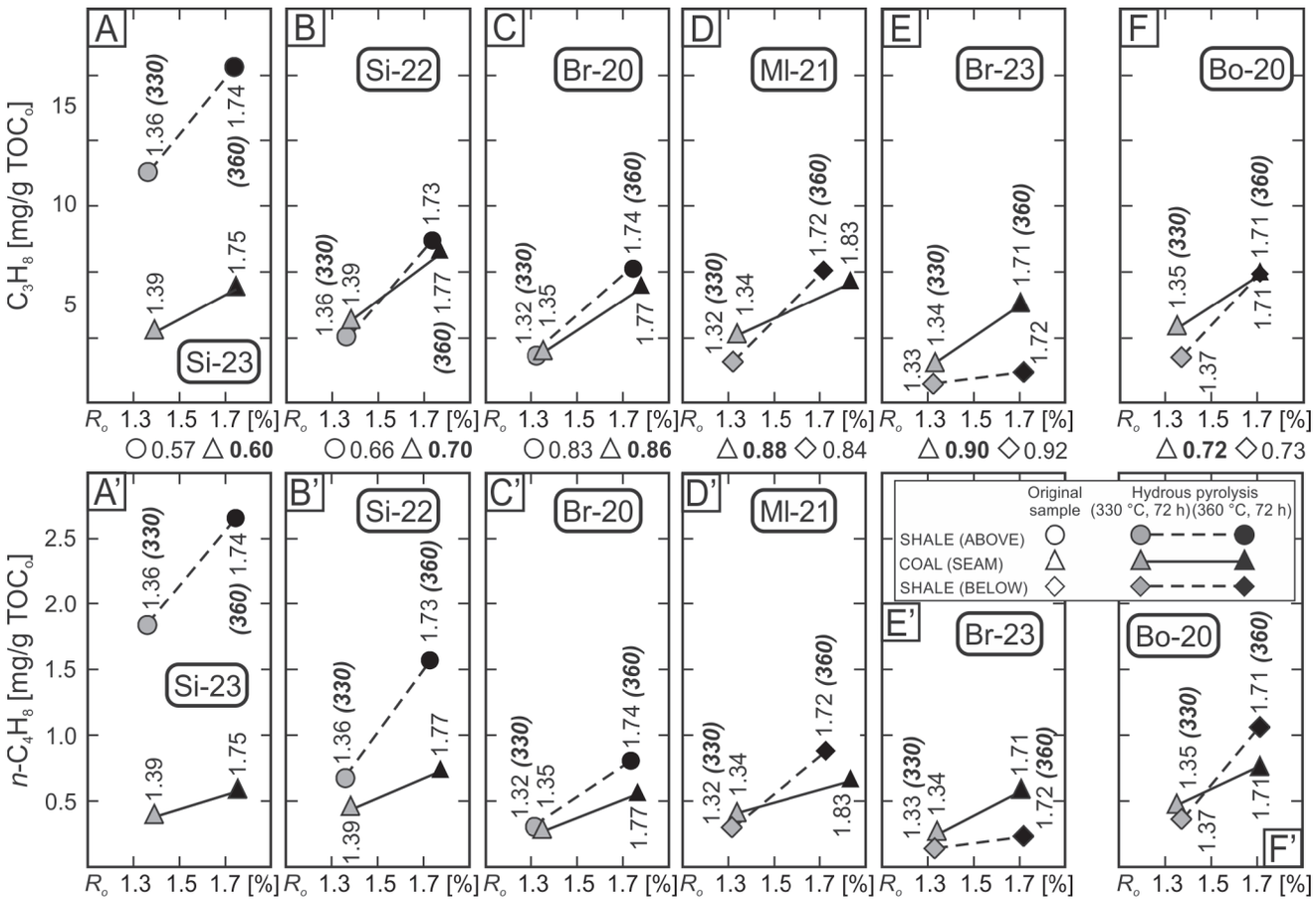

Fig. 10. Yields of propane (A to F in upper row) and *n*-butane (A' to F' in lower row) generated from coals and carbonaceous shales of Si-23 (A and A'), Si-22 (B and B'), Br-20 (C and C'), MI-21 (D and D') and Br-23 (E and E') samples of the Upper Silesian Coal Basin, and Bo-20 sample of the Lublin Coal Basin (F and F') *versus* vitrinite reflectance after HP experiments at 330 and 360°C

Vitrinite reflectance values for original coal (triangle, bold) and carbonaceous shale (circle or rhomb, normal) are between the upper and lower rows; TOC_o – total organic carbon of original organic matter

(Appendix 3 and Fig. 4). The maturity increase caused by HP at 330 and 360°C ranges from 1.32 to 1.39% (HP maturity: first stage) and from 1.71 to 1.83% (HP maturity: second stage), respectively (Appendix 3 and Fig. 4). A good correlation of parameters and indices of rank, i.e. Rock-Eval T_{max} temperature, C^{daf} content, atomic H/C ratio, VM^{daf} with R_o, and a larger scatter of their values for carbonaceous shales as compared to coals (Appendices 3 and 4, Fig. 4) suggests a greater heterogeneity of dispersed organic matter and probably an insignificant admixture of algal (mixed III/II type) macerals. This evaluation is consistent with the origin and maturity of the organic matter based on petrographic and geochemical studies as described earlier by Kruszewska (1983), Gabzdyl and Probierz (1987), Ptak and Różkowska (1995), Jurczak-Drabek (1996), Matuszewska (2002), Kotarba et al. (2002), Kotarba and Clayton (2003), Ćmiel (2012), Fabiańska et al. (2013) and Misiak (2017) in USCB and Grotek et al. (1998), Kotarba et al. (2002), Kotarba and Clayton (2003) and Grotek (2007) in the LCB as well as in Carboniferous profiles of the Chełmek IG 1 (Janas, 2018; Jureczka, 2018) and Ruptawa IG 1 boreholes (Jurczak-Drabek, 2015; Kozłowska et al., 2015) in the study area of the USCB (Fig. 1C) and Busówno IG 1 (Grotek, 2007) in the study area of the LCB (Fig. 1B).

HP experiments simulate natural coalification during which maturity increase in the organic matter of coals and shales was accompanied by gas generation.

GAS GENERATED DURING HP EXPERIMENTS

HYDROCARBON GASES

The yields of methane, ethane, propane and *n*-butane generated from coals and carbonaceous shales almost always show very similar trends at the same temperature conditions (Figs. 7, 8A, B, 9 and 10). However, some distinctive patterns were observed. For example, the carbonaceous shales showed methane and ethane yields higher than from the coals for sample Si-23 both at 330 and 360°C (Fig. 9A, A') and for sample MI-21 at 360°C (Fig. 9D, D'), and also propane and *n*-butane yields in the case of samples Si-22 and Br-20 at both 330 and 360°C (Fig. 10B, B', C, C'). Moreover, the yields of methane both from the coals and carbonaceous shales were always higher than the sum of higher gaseous hydrocarbons ([C_2H_6 to C_4H_{10}]) (Fig. 7). Methane and higher gaseous hydrocarbon yields (Fig. 7) and the C_{HC} index (Fig. 5A'–C') of the Si-23st shale sample were much higher in the first case and lower in the second than in other carbonaceous shale and coal samples (Figs. 9A, A' and 10A, A'). However, atomic H/C ratios of both dispersed organic matter in the original carbonaceous shales and kerogen in the original coals do not correlate with the hydrocarbon yields (Fig. 8).

The ^{13}C of CH_4, C_2H_6, C_3H_8 and *n*-C_4H_{10} *versus* their reciprocal carbon-number are plotted on Figure 11. HP thermogenic

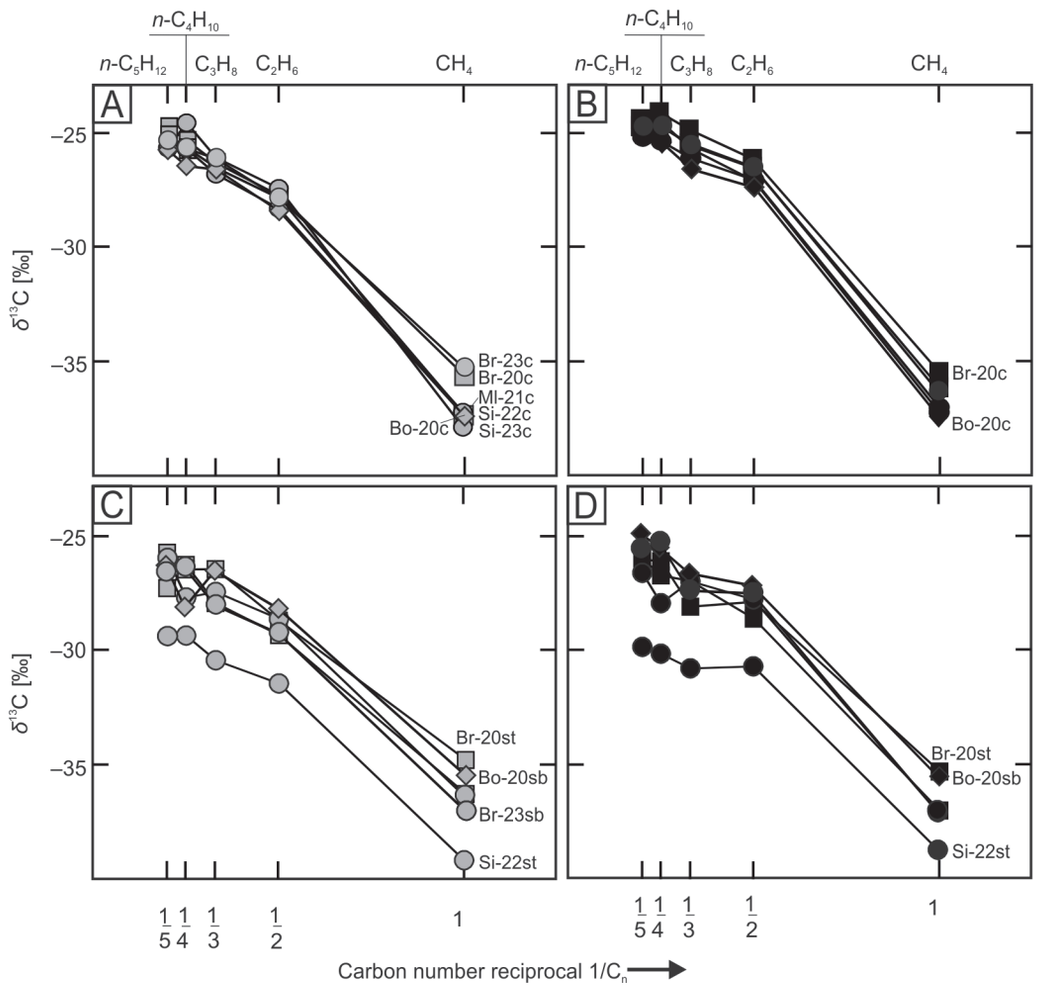

Fig. 11. Stable carbon isotope composition of methane, propane, *n*-butane and *n*-pentane *versus* the reciprocal of their carbon number generated from coals (A and B) and carbonaceous shales (C and D) of the USCB and LCB during HP at (A and C) 330 and (B and D) 360°C

Order of ^{13}C values for CH_4, C_2H_6 and C_3H_8 after Chung et al. (1988); for key to stratigraphy of currently analysed samples and type of HP experiment see Figure 7

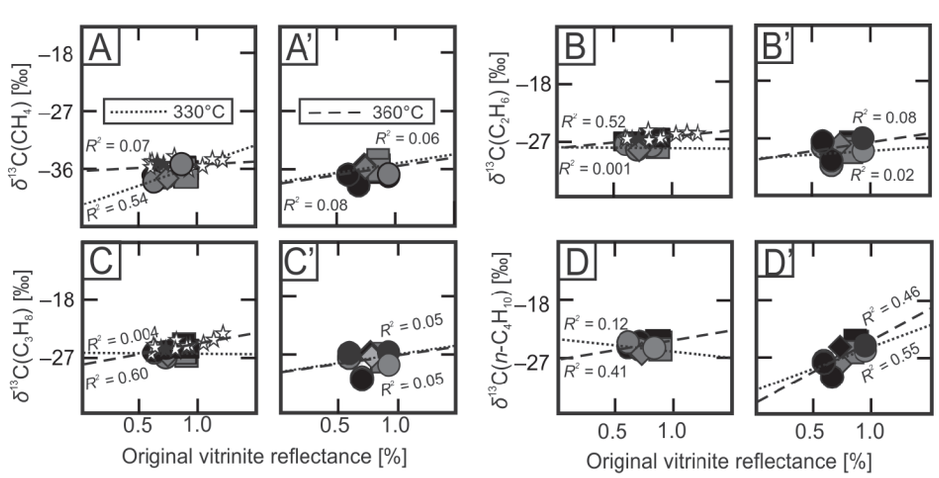

Fig. 12. Stable carbon isotope composition of methane (A), ethane (B), propane (C) and *n*-butane (D) generated from coals, and methane (A'), ethane (B'), propane (C') and *n*-butane (D') generated from carbonaceous shales during the HP experiments *versus* original vitrinite reflectance

Dotted and dashed lines for 330 and 360°C HP gases, respectively. Data for currently analysed coals and carbonaceous shales are from Appendices 2 and 6, and coals marked by open stars are after Kotarba and Lewan (2004) and Lewan and Kotarba (2014); for key to stratigraphy of currently analysed samples and type of HP experiment see Figure 7

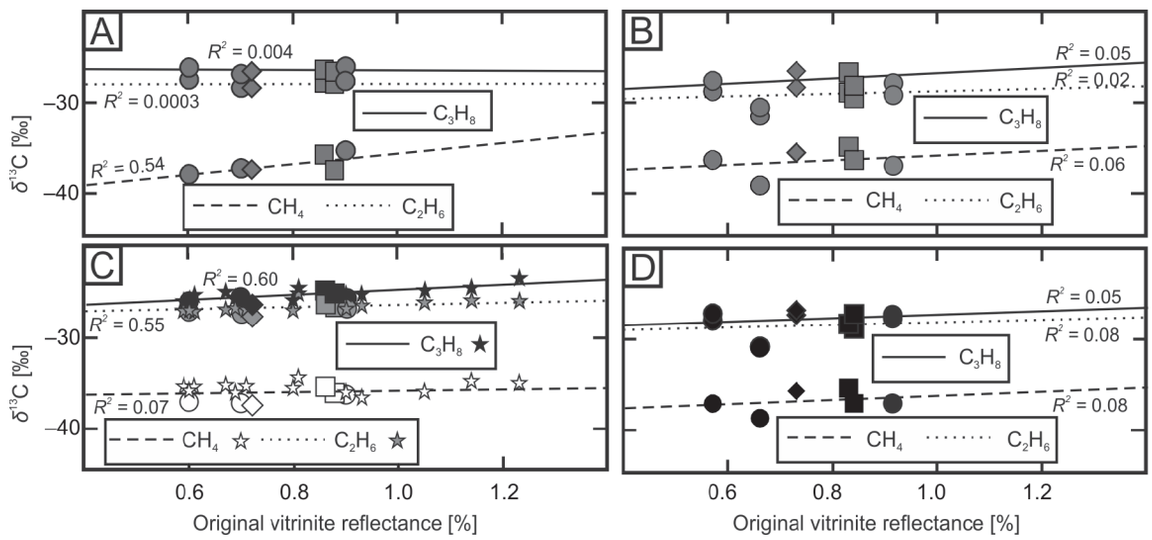

Fig. 13. Stable carbon isotope composition of methane, ethane and propane *versus* original vitrinite reflectance for HP gases generated at 330 and 360°C, respectively, from coals (A and C) and carbonaceous shales (B and D)

Data for currently analysed coals and carbonaceous shales are from Appendices 2 and 6. For comparison, onto (C) are added data for coals from the Upper Silesian and Lublin basins after Kotarba and Lewan (2004) and Lewan and Kotarba (2014): methane – open star, ethane – grey star, propane – black star; for key to stratigraphy of currently analysed samples and type of HP experiment see Figure 7

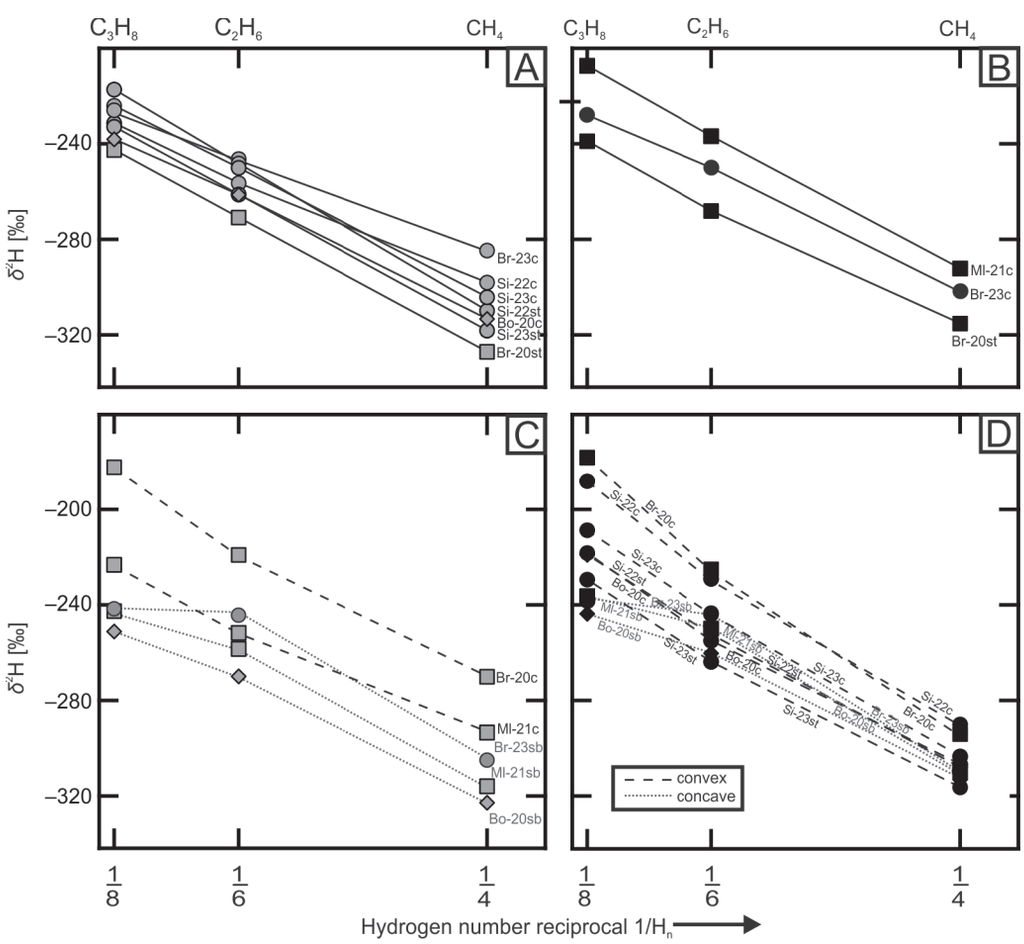

Fig. 14. Stable hydrogen isotope composition of methane, ethane and propane of linear trends (A and B) and convex and concave trends (C and D) for HP gases analysed after experiments at 330°C (A and C)and at 360°C (B and D) *versus* the reciprocal of their hydrogen number

For key to stratigraphy of currently analysed samples and type of HP experiment see Figure 7

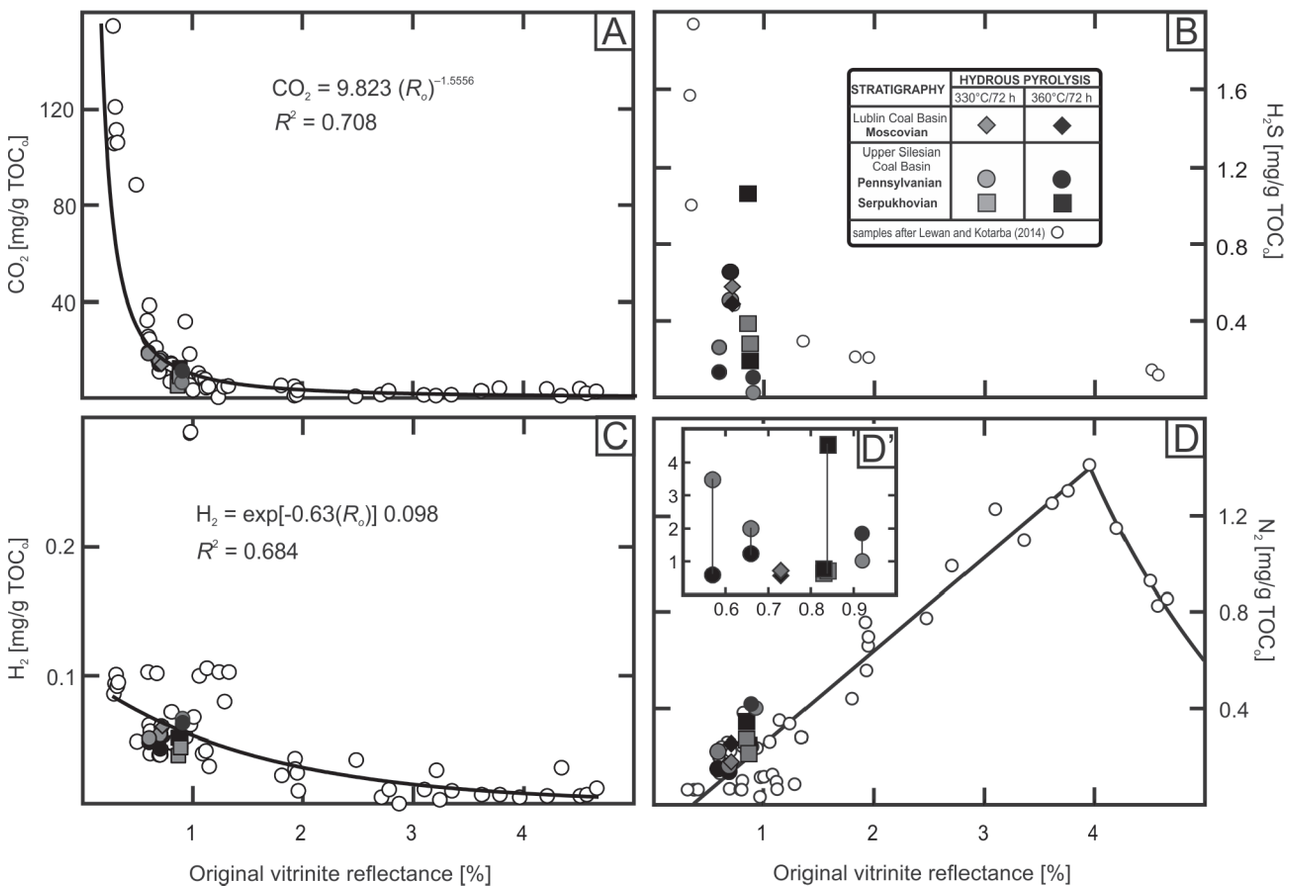

Fig. 15. Yields of carbon dioxide (A), hydrogen sulphide (B), molecular hydrogen (C) and molecular nitrogen generated from coals (D) and carbonaceous shales (D') analysed by HP at 330 and 360°C in comparison with HP gases (after HP at 360°C) expelled from different coal samples from Northern Hemisphere basins (Lewan and Kotarba, 2014) *versus* of vitrinite reflectance of original coals (A, B and C) and currently analysed original carbonaceous shales (D')

Trend lines on (A) and (C) shows the best fit for results obtained in the present study and for previously published data after Lewan and Kotarba (2014) and on (D) based on vitrinite reflectance of original coals (Appendix 2) and N_2 yield from coals after HP at 360°C (Appendix 6) and Lewan and Kotarba (2014); TOC_o – total organic carbon of original organic matter

gases generated from the coals and carbonaceous shales show a mostly convex-concave (dogleg) pattern (Fig. 11). HP thermogenic gases do not have to follow a linear trend as previously suggested (Chung et al., 1988).

The values of stable carbon isotope composition of CH_4, C_2H_6, C_3H_8 and *n*-C_4H_{10} generated from the carbonaceous shales by HP at 330 and 360°C (Fig. 12A'–D'), from the coals by HP at 360°C (Fig. 12A–D) and CH_4 from the coals by HP at 330°C (Fig. 12A) correlate positively with the original vitrinite reflectance (R_o) values. C_2H_6, C_3H_8 and *n*-C_4H_{10} (Fig. 12B, C, D) generated from the coals during HP at 330°C are depleted in the ^{13}C isotope with increasing maturity. A similar isotope trend was observed for HP gases of coals from Northern Hemisphere (Germany, Poland, Ukraine and USA) basins by Lewan and Kotarba (2014) and for coalbed gases reported or modeled by various investigators for type-III kerogen as compiled by Whiticar (1994).

The ^{13}C values of CH_4, C_2H_6 and C_3H_8 generated from coals at 360°C (Fig. 13C) and from carbonaceous shales at 330 and 360°C (Fig. 13B, D), and C_2H_6 and C_3H_8 from coals at 330°C (Fig. 13A) show insignificant changes with increasing maturity. Higher ^{13}C enrichment of methane during increasing rank of coal was observed (Fig. 13A).

^{2}H-depleted methane can be explained by the ^{2}H-depleted distilled water (–66‰, Appendix 7) from water of the Kraków pipe network used in the HP experiments, of isotopic composition typical of Kraków-area precipitation (Duliński et al., 2019), which is also reflected in the recovered waters with ^{2}H values varying from –72 to –52‰ (Appendix 7 and Fig. 6B). In previous HP experiments performed for coals from the USCB and LCB at 360°C for 72 hours Denver distilled water of ^{2}H ratio of –108‰ was used and the recovered waters had ^{2}H values from –95 to –91‰ (Kotarba and Lewan, 2004; Fig. 6B). The process of generation of ^{2}H-depleted methane during hydrous pyrolysis of source rocks from the Polish petroleum basins was previously discussed by Kotarba and Lewan (2013) and Kotarba et al. (2009). Three hydrogen atoms in CH_4 are from methyl radicals of organic matter with one atom from water. Five hydrogen atoms in C_2H_6 are from ethyl radicals of organic matter with one atom from water. Seven hydrogen atoms in C_3H_8 are from propyl radicals of organic matter with one atom from water. The ability of water to be a source of hydrogen during the thermal cracking of hydrocarbons has been shown experimentally (Hoering, 1984; Lewan, 1997; Schimmelmann et al., 1999, 2001). Unlike the importance of kerogen influencing ^{13}C values for generated hydrocarbon gases, ^{2}H values of hydrocar-

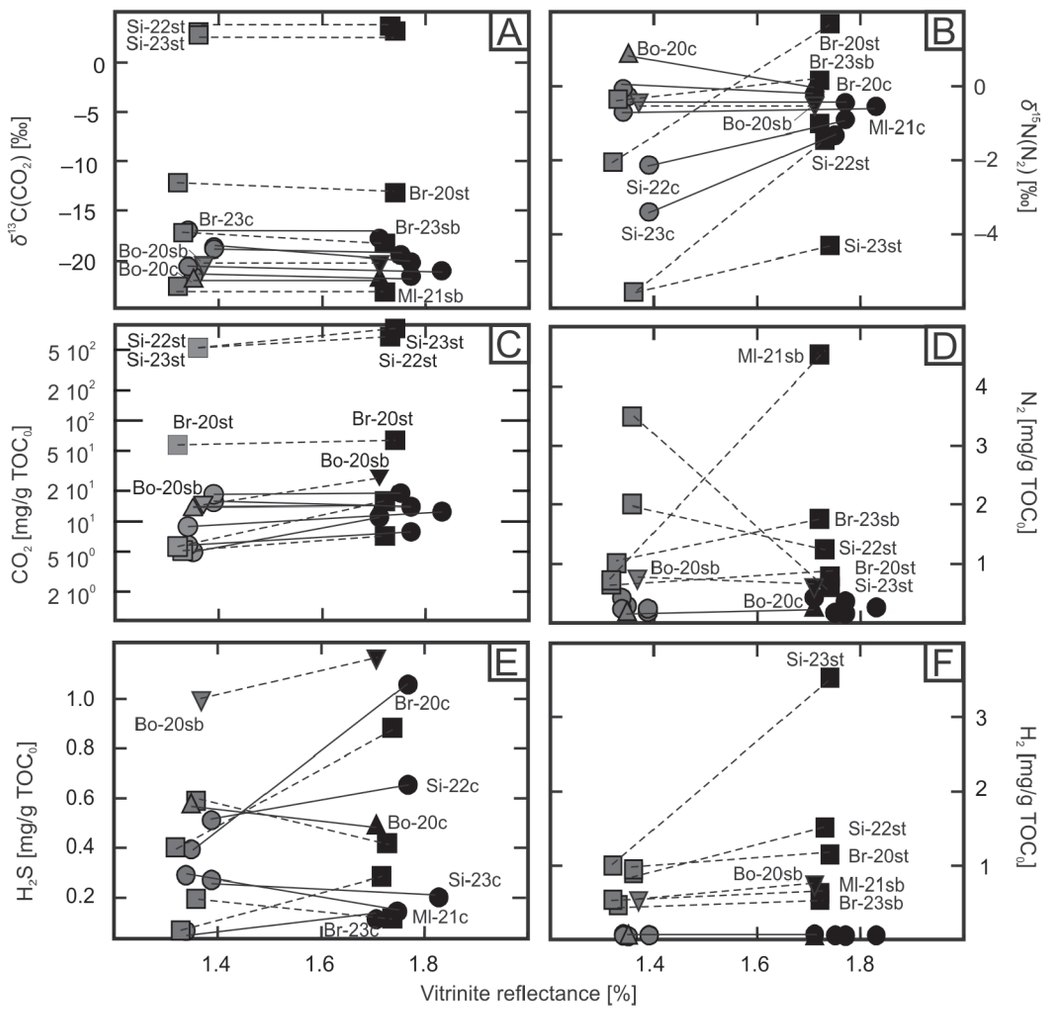

Fig. 16. Stable isotope compositions of carbon (A) in carbon dioxide and nitrogen (B) in molecular nitrogen, and yields of carbon dioxide (C), molecular nitrogen (D), hydrogen sulphide (E) and molecular hydrogen (F) expelled from coals and carbonaceous shales analysed by HP at 330 (grey marks) and 360°C (black marks)

Solid and dashed lines link gases generated from the same coal and carbonaceous shale samples, respectively; for sample keys and stratigraphy of analysed samples see Appendix 1 and Figure 15

bon gases can be influenced by the formation waters present in a source rock during their generation in a natural environment (e.g., Smith et al., 1982, 1985). ^{2}H differences between Kraków and Denver distilled and recovered waters are 42‰ and 19–43‰, respectively (Fig. 6B), therefore the difference between the ^{2}H of methane generated from coals from the USCB and LCB in Kraków during 72 hrs HP at 360°C (–308 to –290‰, Appendix 6), compared with the Denver laboratory results (–319 to –302‰, Kotarba and Lewan, 2004), is 11–12‰, one-fourth of these values (Fig. 6B). The ^{2}H values of CH_4, C_2H_6 and C_3H_8 versus their reciprocal hydrogen-number are shown in Figure 14. The HP gases generated from the coals and carbonaceous shales have both linear (Fig. 14A, B) and convex-concave (dog-leg) relationships (Fig. 14C, D). Similar trends have been observed in natural gases from petroleum basins in China (Ni et al., 2019a, b), and Poland and Ukraine (Kotarba et al., 2019b, 2020a, b; Bilkiewicz and Kowalski, 2020; Więcław et al., 2020).

The HP thermogenic and coalbed gases from the USCB and LCB are compared on Figures 6, 18 and 20. These comparisons show that the coalbed gases in the USCB and LCB have a significant microbial component, or this isotopic fractionation (shift) can be related to physicochemical sorption/desorption and diffusion processes during migration through microporous coals (Kotarba, 2001).

NON-HYDROCARBON GASES

Carbon dioxide (CO_2), hydrogen sulphide (H_2S), molecular hydrogen (H_2) and molecular nitrogen (N_2) are the main non-hydrocarbon gases generated during HP experiments. The concentrations of these gases, gas indices and stable isotope composition of carbon dioxide and molecular nitrogen are shown in Appendices 5 and 6. The unusually large yields of CO_2, H_2 and H_2S generated in HP (Appendix 8), as compared to a natural system, may be partly explained by the high temperatures of hydrous pyrolysis that result in increasing fugacities for each gas component (Cooles et al., 1987) and additionally influences secondary processes during migration in the geological environment. In the natural system, highly soluble H_2S and CO_2, and reactive H_2, may be lost by dissolution, adsorption and migration processes (e.g., Hunt, 1996). N_2 practically does not un-

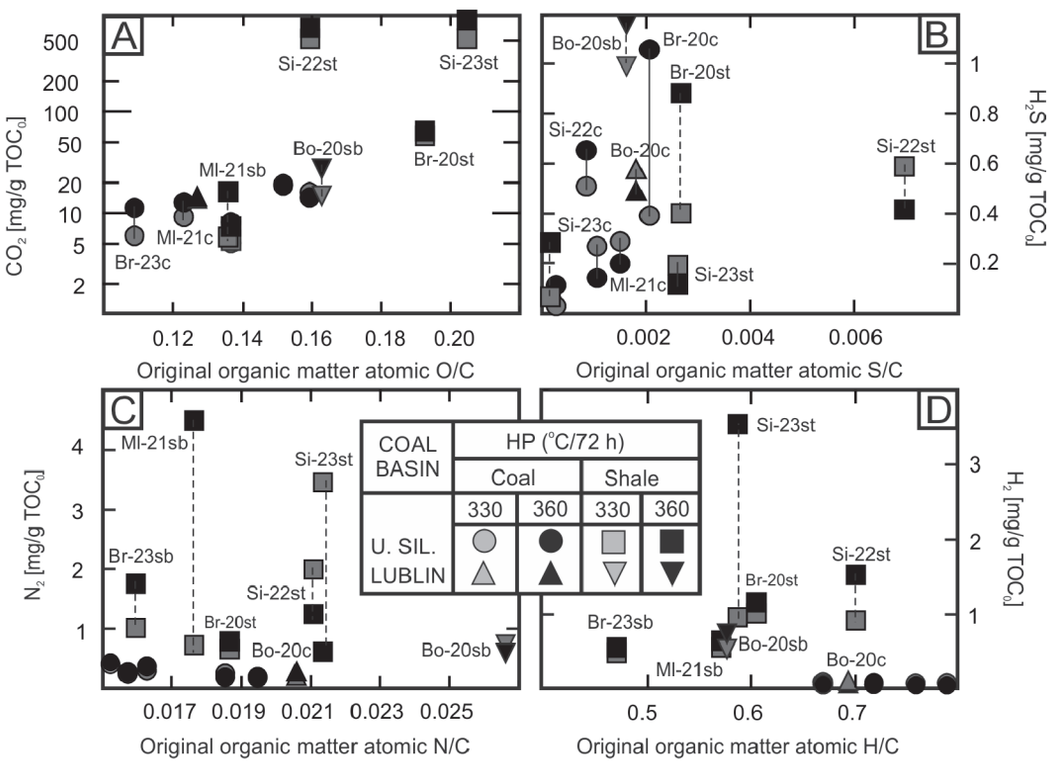

Fig. 17. Non-hydrocarbon gas yields of carbon dioxide (A), hydrogen sulphide (B), molecular nitrogen (C) and molecular hydrogen (D) expelled from coals and carbonaceous shales analysed during HP at 330 and 360°C *versus* the atomic ratios of O/C (A), S/C (B), N/C (C) and H/C (D) of their original kerogen

U. SIL. – Upper Silesian

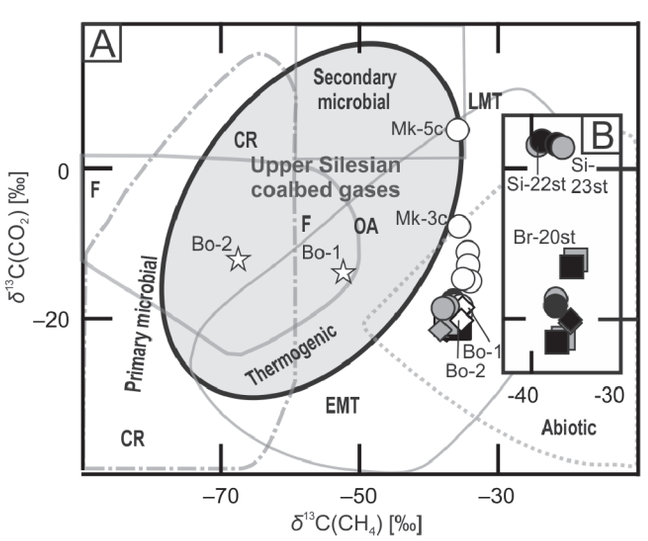

Fig. 18. Stable carbon isotope composition of carbon dioxide *versus* stable carbon isotope composition of methane for HP gases expelled from coals (A) and carbonaceous shales (B)

Genetic fields after Milkov and Etiope (2018); for comparison, Upper Silesian (shaded field) and Lublin (Bo-1 and Bo-2 open stars) coalbed methane and carbon dioxide after Kotarba (2001) and Kotarba and Pluta (2009), and Upper Silesian and Lublin (Bo-1 and Bo-2) HP at 360°C gases after Kotarba and Lewan (2004) and Lewan and Kotarba (2014) are also shown: for key to gas sample codes and stratigraphy of currently analysed and previously published gas samples see Figures 7 and 17, respectively

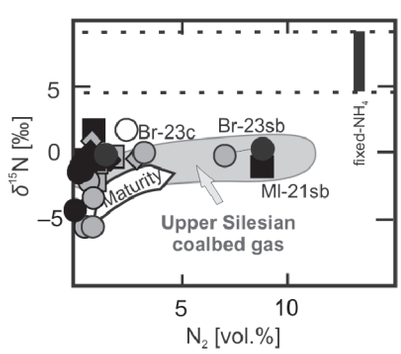

Fig. 19. Stable nitrogen isotope composition of N_2 *versus* N_2 concentration for currently analysed HP gases

Direction of source rock maturity after Gerling et al. (1997) and range of fixed-NH_4 after Mingram et al. (2005); for comparison, Upper Silesian coalbed molecular nitrogen after Kotarba (2001); for key to gas sample codes and stratigraphy of currently analysed samples see Figure 17

dergo secondary processes therefore its yield (Appendix 8) remains the same.

Carbon dioxide. A common feature of HP experiments is the production of large quantities of carbon dioxide (e.g., Andresen et al., 1994; Lewan, 1997; Kotarba and Lewan, 2004; Lewan and Kotarba, 2014). The intensity and dynamics of CO_2 generation during HP decrease with increasing maturity of the coals (Fig. 15A) and are higher for carbonaceous shales than for coals (Appendix 8 and Fig. 16C). Decarboxylation is due to the weaker C–O bond strength as compared to that of the C–C

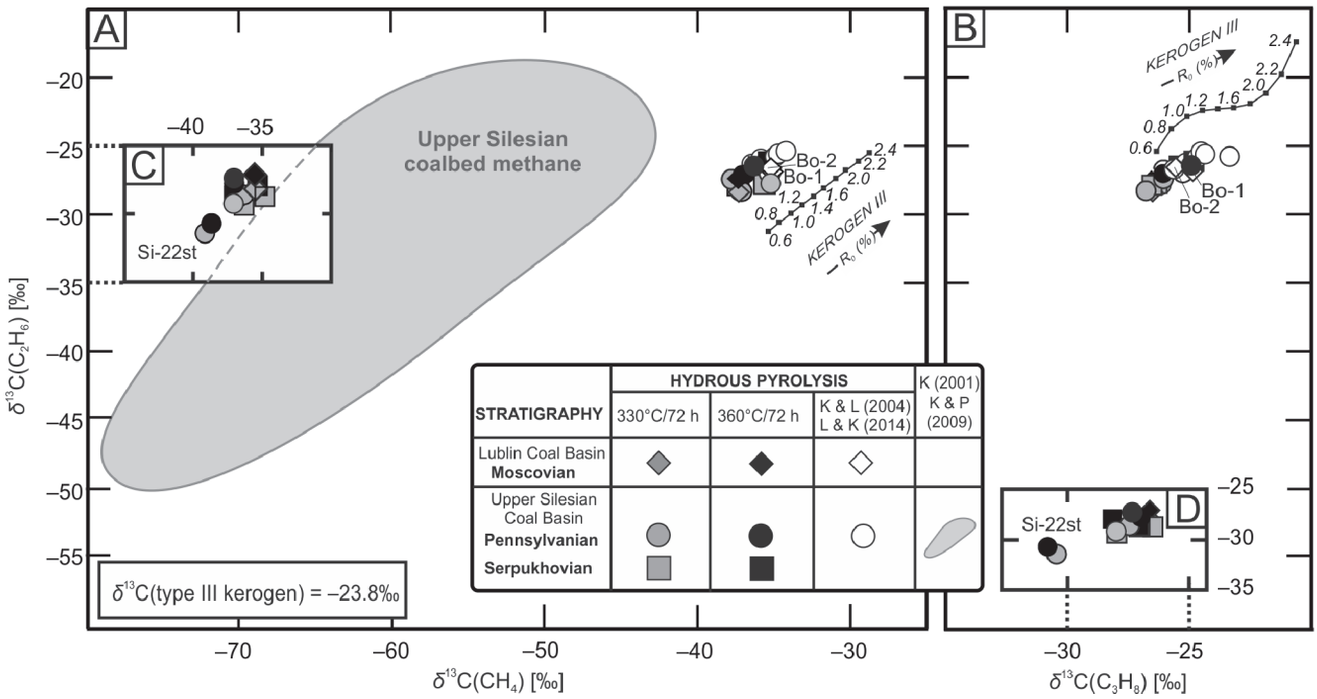

Fig. 20. Stable carbon isotope composition of ethane *versus* stable carbon isotope composition of methane (A and C) and stable carbon isotope composition of propane (B and D) of HP gases expelled from coals (A and C) and carbonaceous shales (C and D)

Position of reflectance curves for type-III kerogen after Berner and Faber (1996) shifted based on average of ^{13}C value (–23.8‰, 24 samples) of Serpukhovian and Pennsylvanian coals from the Upper Silesian and Lublin basins (Kotarba and Clayton, 2003); for comparison, Upper Silesian coalbed gases (shaded field) after Kotarba (2001) [K (2001)] and Kotarba and Pluta (2009) [K & P (2009)], and the Upper Silesian and Lublin (Bo-1 and Bo-2) HP gases after experiments at 360°C for 72 hours from coals after Kotarba and Lewan (2004) [K & L (2004)] and Lewan and Kotarba (2014) [L & K (2014)] are also shown

bond (Kotarba, 1988; Hunt, 1996). Moreover, during thermal transformation of humic organic matter the thermodynamic effect of isotope fractionation is dominant and the carbon dioxide generated is enriched in ^{13}C by 12–28‰ as compared to source humic source matter (Galimov, 1985). The volume of carbon dioxide generated is proportional to the atomic O/C ratio (i.e., oxygen content) of the initial organic matter while its quantity is greater in shales than in coals (Fig. 17A) reaching a maximum yield of 817 mg/g TOC_o and only 18.9 mg/g TOC_o for carbonaceous shales and coals, respectively (Appendix 8). The ^{13}C values of CO_2 do not show substantial variations between gases generated from the same initial samples, but remarkable differences are seen among gases generated from different initial samples. The isotopic differentiation observed is related to genetic features of the source material of CO_2, not to maturation processes induced by HP. Negative ^{13}C values of most of the samples analysed indicate that the CO_2 was generated from thermal decomposition of organic matter (Fig. 18). Extreme high CO_2 yields were obtained for two carbonaceous shale samples: Si-22st and Si-23st, and only in these samples does the CO_2 show positive ^{13}C values (Appendices 6 and 8). High yields accompanied by notably high ^{13}C values of CO_2 indicate that the CO_2 in these samples was generated from a different source material than in remaining samples, most likely containing more organic molecules with C-O functional groups or, less probably, was produced from carbonate dissolution/decomposition, while the release of pre-existing carbon dioxide adsorbed or entrapped in the initial samples cannot be excluded. Mineral carbon measured in the samples studied does not support the hypothesis of the influence of carbonate minerals, since its content in samples Si-22st and Si-23st is neither higher than in other samples nor was greatly decreased (Appendix 3). The different isotopic compositions of gases generated from samples Si-22st and Si-23st may be related to their lower initial maturity and a higher content of oxygen compounds such as organic acids contributing to ^{13}C enriched CO_2. In addition to decarboxylation, some of the oxygen in the CO_2 generated by hydrous pyrolysis has been shown to be derived from water interacting with the carbonyl groups (Lewan, 1997; Lewan and Kotarba, 2014). CDMI values, showing the relation of generation of CO_2 to CH_4, decrease with increasing original vitrinite reflectance of pyrolysed organic matter and also with increasing HP temperature (Appendix 6 and Fig. 5A–C), indicating that the maximum yield for CO_2 occurs at lower maturity than that for CH_4 and that CO_2 from coals was liberated less effectively.

Hydrogen sulphide. During maturation of sedimentary organic matter, large amounts of hydrogen sulphide may be generated (e.g., Orr, 1977; Anissimov, 1995; Amrani et al., 2005).

No correlations exist between H_2S yields and the R_o and original organic matter atomic S/C ratio of the coals analysed (Figs. 15B, 16E and 17B). This may be explained by the original sulphur occurring in different organic compounds (e.g., thiols, sulphides, and thiophenes; Chou, 1990), which have different thermal stabilities and yield different amounts of H_2S. Thiols and sulphides are the most likely source of H_2S because their carbon-sulphur bonds are weaker than those in aromatic thiophene rings (Lewan and Kotarba, 2014). The rank of the original coals, represented by R_o, is narrow, i.e. from 0.6 to 0.9% (Appendix 3). The broad rank from lignites to anthracites, as observed by Lewan and Kotarba (2014), also does not re-

veal such correlations. Only lignites have some of the high yields (Fig. 15B). H_2S yields from the organic matter of carbonaceous shales are comparable to those from coals, while the greatest yields were observed from shale sample Si-23st (Appendix 8, Figs. 16E and 17B) which may be associated with the composition of sulphur compounds as well as with a catalytic and adsorbed influence of the claystone-mudstone matrix. Similarly to CO_2, significant concentrations of H_2S can occur as dissolved aqueous species depending on solution pH (e.g., Lewan, 1997). Although hydrogen sulphide was generated in large volumes from the coals and carbonaceous shales during the HP experiments, no traces of it are found in coalbed gas accumulations within the Carboniferous coalbed strata of the Polish basins (Kotarba, 1990a, b, c, 2001; Kotarba and Rice, 2001; Kotarba and Pluta, 2009). This absence of hydrogen sulphide as a free gas is attributed to its high solubility in formation waters and its high reactivity with Fe and other transition metals (i.e., Cu, Pb and Zn) during gas migration and entrapment (e.g., Orr, 1977; Suleimenov and Krupp, 1994). The major removal process of H_2S in clastic and claystone–sandstone successions of the coalbed strata appears to be caused by the formation of pyrite and other metal sulphides.

Molecular hydrogen. Molecular hydrogen was also expelled in notable quantities from coals and in considerable amounts from carbonaceous shales during the HP experiments for 72 hours at 330 and 360°C (Appendix 8, Figs. 15C, 16F and 17D). However it may rarely occur in traces (if at all) in coalbed gases accumulated within the Carboniferous strata of the USCB and LCB (Kotarba, 2001; Kotarba and Pluta, 2009). H_2 is very reactive, mobile and practically not subject to adsorption on coals, so its retention in coal-bearing strata is ephemeral (Lewan and Kotarba, 2014). The dual source of H_2 from water and organic matter and its participation with H_2S generation makes its behaviour complex to interpret from the HP experiments of this study.

As in the case of sulphide hydrogen (Figs. 15B and 17B), H_2 yields decrease with increase in maturity (Fig. 15C) and with the increasing atomic H/C ratio of the original kerogens of both the coals and carbonaceous shales (Fig. 17D). These phenomena are mainly caused by expelling hydrogen from organic matter during maturation. H_2 was also generated in considerable quantities from water and the organic matter of coals and in larger amounts from shales (Figs. 16F and 17D). Early-generated H_2 is scavenged to make H_2S, which forms early and in high quantities from type-III kerogen in HP experiments (Figs. 15C and 16F).

Molecular nitrogen. Molecular nitrogen in natural, geological environments is produced in large quantities in radiogenic, atmospheric, primordial, crustal and organic processes (including microbial processes and the thermogenic decomposition of organic matter) (e.g., Jenden et al., 1988; Krooss et al., 1995, 2008; Gerling et al., 1997; Kotarba et al., 2014, 2019a, 2020c). N_2 can be also released from NH_4-rich illites that have undergone intensive fluid/rock interaction (Lüders et al., 2005; Mingram et al., 2005).

During our HP experiments, N_2 was generated from nitrogen compounds in the organic matter of the coals and shales, and from NH_4-rich illites of the shales. N_2 yields increase continuously with increase in R_o of the original samples, from 0.6 to 1% (Fig. 17C). This is in agreement with the observation of Lewan and Kotarba (2014), who reported N_2 generation rise as R_o of original samples increased from 0.4 up to 4%, then a sudden drop at higher maturities (Fig. 15D). The original increase in molecular nitrogen as opposed to the overall decrease in CO_2, H_2S and H_2 with increasing original R_o of the coals can be explained by differences in their covalence (Fig. 15). In addition to organically bound nitrogen, some of the nitrogen yields may be derived from ammonium in clay minerals (Mingram et. al., 2005) or N_2-bearing fluid inclusions (Lüders et al., 2005, 2012) in the coals and carbonaceous shales.

Isotopic fractionation depends on the primary genetic factors of the organic matter, and the secondary processes taking place during gas migration through the gas-rock and gas-reservoir fluid interfaces (Littke et al., 1995; Krooss et al., 1995, 2005, 2008; Gerling et al., 1997; Zhu et al., 2000; Mingram et al., 2005; Lüders et al., 2005). Molecular nitrogen generation from organic matter has been also documented during pyrolysis experiments (Gerling et al., 1997; Kotarba and Lewan, 2004, 2013; Lewan and Kotarba, 2014). In most cases molecular nitrogen generated during our 360°C HP experiments is more enriched in the ^{15}N isotope than that from the 330°C HP experiments, both from coals and carbonaceous shales (Appendix 6, Figs. 16B and 19). The NH_4-fixed in claystones and mudstones is enriched in ^{15}N as compared with nitrogen compounds in organic matter (e.g., Gerling et al., 1997; Mingram et al., 2005; Krooss et al., 2008) hence the observed nitrogen isotope fractionation (Figs. 16B and 19) is probably connected with increasing N_2 yields, rising coal maturity (Fig. 15D) and additional N_2 generation from fixed-NH_4 compounds within claystones (Fig. 15D').

CONCLUSIONS

Hydrous pyrolysis (HP) experiments at 330 and 360°C for 72 hours were carried out on Serpukhovian, Bashkirian and Moscovian coals and carbonaceous shales from the USCB (10 samples) and the LCB (2 samples). The samples were selected based on the results of Rock-Eval-II pyrolysis of 28 coal and 55 shale samples. The results and interpretations of the organic geochemical and petrographic screening analyses with regard to the origin and maturity of the organic matter before and after the HP experiments, and the yields, and molecular and stable carbon, hydrogen and nitrogen isotope compositions of the gases generated during HP can be summarized as follows:

1. R_o of the humic (type-III kerogen) coals and the carbonaceous shales selected for this study ranged from ~0.60 to 0.90%. After 72 h HP at 330°C (first stage of artificial maturation) R_o had increased to ~1.3–1.4% and after 72 h HP at 360°C (second artificial maturation stage) to ~1.7–1.8% (cf. Appendix 3, Figs. 4, 9 and 10);
2. The hydrocarbon gases (CH_4, C_2H_6, C_3H_8 and n-C_4H_{10}) generated from the carbonaceous shales at 330 and 360°C showed an enrichment in ^{13}C with increasing R_o of the original samples. The same trend was observed for the C_1 to C_4 hydrocarbons generated from coals by HP at 360°C. For the HP of coals at 330°C this trend was only observed for methane while the C_2 to C_4 hydrocarbons showed a depletion in ^{13}C with increasing original maturity (cf. Appendix 6 and Fig. 11);
3. ^{2}H-depleted methane can be explained by the ^{2}H-depleted distilled water (–66‰) in water of the Kraków pipe network used in the HP experiments, which is also reflected in the recovered waters with ^{2}H values varying from –72 to –52‰ (cf. Appendices 6 and 7, Figs. 6B and 14);
4. The plots of the ^{13}C values of the hydrocarbon gases generated, CH_4, C_2H_6, C_3H_8 and n-C_4H_{10}, *versus* their reciprocal carbon-number (Chung plots) are not linear but have concave (dog-leg) shapes (cf. Appendix 6 and Fig. 11);

5. The ^{2}H of CH_4, C_2H_6 and C_3H_8 in HP gases *versus* their reciprocal hydrogen-number have both linear and convex-concave (dog-leg) relationships (cf. Appendix 6 and Fig. 14);
6. The broad fractionation of ^{13}C values of carbon dioxide can be caused by both kinetic and thermodynamic effects related to thermal organic matter destruction. The picture of distribution of ^{13}C values of HP carbon dioxide is similar to the distribution of its yields, although somewhat reversed trends with changes in vitrinite reflectance were observed (cf. Appendices 6 and 8, Figs. 16C and 18);
7. No correlations exist between hydrogen sulphide yields and either vitrinite reflectance or original organic matter atomic S/C ratio in the coals analysed. H_2S yields of organic matter of shales are comparable to those from coals, which may be associated with the composition of sulphur compounds as well as with the catalytic and adsorbed influence of the claystone-mudstone matrix (cf. Appendix 8, Figs. 15B, 16E and 17B);
8. Molecular hydrogen was generated in significant quantities from water and the organic matter of the coals and in considerable amounts from shales during the HP experiments at 330 and 360°C. The decreasing trend in H_2 yields with a decrease in maturity and the increasing atomic H/C ratio of the original kerogens of coals and shales hold to the value of ~0.6 (cf. Appendices 6 and 8, Figs. 15C, 16F and 17D);
9. During our HP experiments, molecular nitrogen yields increase with increasing vitrinite reflectance of the original coals and carbonaceous shales. In most cases molecular nitrogen generated in the 360°C HP experiments is more enriched in ^{15}N than in N_2 generated during the 330°C HP experiments both from coals and shales (cf. Appendices 5, 6 and 8, Figs. 15D, 16D and 19).

Acknowledgements. This research was undertaken as part of Polish National Science Centre support under grant no. UMO-2016/22/M/ST10/00589 (AGH University of Science and Technology, no. 28.28.140.70320). We would like to express our gratitude to A.V. Milkov from the Colorado School of Mines in Golden, Y.V. Koltun from the Institute of Geology and Geochemistry of Combustible Minerals of the National Academy of Sciences of Ukraine in Lviv and two anonymous reviewers for their constructive comments and suggestions, which improved an earlier version of the manuscript. Sample collecting and experimental and analytical works by A. Kowalski, T. Kowalski, N. Kmiecik and T. Romanowski from the AGH University of Science and Technology in Kraków is gratefully acknowledged.

REFERENCES

Andresen, B., Throndsen, T., Barth, T., Bolstad, J., 1994. Thermal generation of carbon dioxide and organic acids from different source rocks. Organic Geochememistry, **21**: 1229–1242.

Andresen, B., Throndsen, T., Raheim, A., Bolstad, J., 1995. A comparison of pyrolysis products with models for natural gas generation. Chemical Geology, **126**: 261–280.

Anissimov, L., 1995. Origin of H_2S in natural gases: identification of geochemical processes. In: Organic Geochemistry: Developments and Applications to Energy, Climate, Environment and Human History (eds. J.O. Grimalt and C. Dorronsoro): 1113–1114. Selected Papers from the 17th International Meeting on Organic Geochemistry Donostia-San Sebastian.

Amrani, A., Lewan, M.D., Aizenshtat, Z., 2005. Stable sulfur isotope partitioning during simulated petroleum formation as determined by hydrous pyrolysis of Ghareb Limestone, Israel. Geochimica et Cosmochimica Acta, **69**: 5317–5331.

ASTM, 2005. American Society For Testing And Materials (ASTM). D2798-05. Standard test method for microscopical determination of the vitrinite reflectance of coal. ASTM International. West Conshohocken, PA.

ASTM, 2011. American Society for Testing and Materials (ASTM). D7708-11. Standard test method for microscopical determination of the reflectance of vitrinite dispersed in sedimentary rocks. ASTM International. West Conshohocken, PA.

Behar, F., Vandenbroucke, M., Tang, Y., Marquis, F., Espitalié, J., 1997. Thermal cracking of kerogen in open and closed systems – determination of kinetic parameters and stoichiometric coefficients for oil and gas generation. Organic Geochemistry, **26**: 321–339.

Berner, U., Faber, W., 1996. Empirical carbon isotope/maturity relationships for gases from algal kerogens and terrigenous organic matter, based on dry, open-system pyrolysis. Organic Geochemistry, **24**: 947–955.

Bilkiewicz, E., Kowalski, T., 2020. Origin of hydrocarbon and non-hydrocarbon (H_2S, CO_2 and N_2) components of natural gas accumulated in the Zechstein Main Dolomite (Ca2) strata in SW part of the Polish Permian Basin: stable isotope and hydrous pyrolysis studies. Journal of Petroleum Science and Engineering, **192**: 107296.

Buła, Z., Kotas, A. (eds.), 1994. Geological Atlas of the Upper Silesian Coal Basin, part III: Structural geological maps 1:100 000 (in Polish with English summary). Państwowy Instytut Geologiczny, Warszawa.

Buła, Z., Żaba, J., 2005. Pozycja tektoniczna Górnośląskiego Zagłębia Węglowego na tle prekambryjskiego i dolnopaleozoicznego podłoża (in Polish). Przew. 76 Zjazdu Pol. Tow. Geol. Rudy k/Rybnika, Warszawa: 14–42.

Chou, C.-L., 1990. Geochemistry of sulfur in coal. American Chemical Society Symposium Series, **429**: 30–52.

Chung, H.M., Gormly, J.R., Squires, R.M., 1988. Origin of gaseous hydrocarbons in subsurface environments: theoretical considerations of carbon isotope distribution. Chemical Geology, **71**: 91–103.

Cohen, K.M., Finney, S.C., Gibbard, P.L., Fan, J.-X., 2013. The ICS International Chronostratigraphic Chart. Episodes, **36**: 199–204.

Cooles, G.P., Mackenzie, A.S., Parkes, R.J., 1987. Non-hydrocarbons of significance in petroleum exploration: volatile fatty acids and non-hydrocarbon gases. Mineral Magazine, **51**: 483–493.

Coplen, T.B., 2011. Guidelines and recommended terms for expression of stable-isotope-ratio and gas-ratio measurement results. Rapid Communications in Mass Spectrometry, **25**: 2538–2560.

Ćmiel, S.R., 2012. Relation between coal transformation and geometric features of faults in the Upper Silesian Coal Basin. Acta Geophysica, **60**: 438–448.

Duliński, M., Różański, K., Pierchała, A., Gorczyca, Z., Marzec, M., 2019. Isotopic composition of precipitation in Poland: a 44-year record. Acta Geophysica, **67**: 1637–1648.

Durand, B., Monin, J.C., 1980. Elemental analysis of kerogen (C, H, O, N, S, Fe). In: Kerogen-Insoluble Organic Matter from Sedimentary Rocks (ed. B. Durand): 113–142. Editions Technip, Paris.

Espitalié, J., Deroo, G., Marquis, F., 1985. La pyrolyse Rock-Eval et ses applications. Revue de l'Institut Francais du Petrole, **40**: 563–579 and 755–784.

Fabiańska, M.J., Ćmiel, S.R., Misz-Kennan, M., 2013. Biomarkers and aromatic hydrocarbons in bituminous coals of Upper Silesian Coal Basin: example from 405 coal seam of the Zaleskie Beds (Poland). International Journal of Coal Geology, **107**: 96–111.

Gabzdyl, W., Probierz, K., 1987. The occurrence of anthracites in an area characterized by lower rank coals in the Upper Silesian Coal Basin of Poland. International Journal of Coal Geology, **7**: 209– 225.

Galimov, E.M., 1985. The Biological Fractionation of Isotopes. Academic Press, London.

Gao, J., Ni, Y., Li, W., Yuan Y., 2020. Pyrolysis of coal measure source rocks at highly to over mature stage and its geological implications. Petroleum Exploration and Development, **47**: 773–780.

Geissler, C., Belau, L., 1971. Zum Verhalten der stabilen Kohlenstoffisotope bei der Inkohlung. Zeitschrift für angewandte Geologie, **17**: 13–17.

Gerling, P., Idiz, E., Everlien, G., Sohns, E., 1997. New aspects on the origin of nitrogen in natural gas in Northern Germany. Geologisches Jahrbuch, **D103**: 65–84.

Grotek, I., 2007. Petrografia i dojrzałość termiczna materii organicznej rozproszonej w osadach paleozoiku (in Polish). Profile Głębokich Otworów Wiertniczych Państwowego Instytutu Geologicznego**, 118**: 134–147.

Grotek, I., **Matyja, H., Skompski, S., 1998.** Thermal maturity of organic matter in the Carboniferous deposits of the Radom–Lublin and Pomerania areas (in Polish with English summary). Prace Państwowego Instytutu Geologicznego, **165**: 245–254.

Higgs, M.D., 1986. Laboratory studies into the generation of natural gas from coals. Geological Society Special Publications, **23**: 113–120.

Hill, R.J., Jenden, P.D., Tang, Y.C., Teerman, S.C., Kaplan, I.R., 1994. Influence of pressure on pyrolysis of coal. ACS Symposium Series, **570**: 161–193.

Hoering, T.C., 1984. Thermal reaction of kerogen with added water, heavy water, and pure organic substances. Organic Geochemistry, **5**: 267–278.

Hunt, J.M., 1996. Petroleum Geochemistry and Geology. W.H. Freeman and Company, New York.

ISO, 2010a. Hard coal and coke – determination of volatile matter. International Standard ISO 562:2010(E). Third edition, Geneva.

ISO, 2010b. Solid mineral fuels – coke – determination of moisture in the general analysis test sample. International Standard ISO 687:2010(E). Third edition, Geneva.

ISO, 2010c. Solid mineral fuels – determination of ash. International Standard ISO 1171:2010(E). Fourth edition, Geneva.

Janas, M., 2018. Badania geochemiczne materii organicznej metodą Rock-Eval (in Polish). Profile Głębokich Otworów Wiertniczych Państwowego Instytutu Geologicznego**, 152**: 211–220.

Jenden, P.D., Kaplan, I.R., Poreda, R.J., Craig, H., 1988. Origin of nitrogen-rich natural gases in the Californian Great Valley: evidence from helium, carbon and nitrogen isotope ratios. Geochimica et Cosmochimica Acta, **52**: 851–861.

Jurczak-Drabek, A., 1996. Petrographic Atlas of the Upper Silesian Coal Basin, 1:300 000 (in Polish with English summary). Państwowy Instytut Geologiczny, Warszawa.

Jurczak-Drabek, A., 2015. Petrografia i jakość węgla (in Polish). Profile Głębokich Otworów Wiertniczych Państwowego Instytutu Geologicznego**, 144**: 121–141.

Jureczka, J., 2018. Wyniki badań litologicznych, stratygraficznych, petrograficznych, mineralogicznych, geochemicznych i chemiczno-technologicznych (in Polish). Profile Głębokich Otworów Wiertniczych Państwowego Instytutu Geologicznego**, 152**: 134–210.

Jureczka, J., Dopita, M., Gałka, M., Krieger, W., Kwarciński, J., Martinec, P., 2005. Geological Atlas of Coal Deposits of the Polish and Czech Parts of the Upper Silesian Coal Basin (in Polish with English summary). Państwowy Instytut Geologiczny, Warszawa.

Jüntgen, H., Karweil J., 1966. Gasbildung und Gasspeicherung in Steinkohleflözen. II. Gasspeicherung. Erdöl und Kohle, Erdgas, Petrochemie, **19**: 339–344.

Jüntgen, H., Klein, J., 1975. Entstehung von Erdgas aus kohligen Sedimenten. Erdöl und Kohle, **28**: 65–73.

Karweil, J., 1966. Inkohlung, Pyrolyse und primäre Migration des Erdöls. Brennstoff-Chemie, **47**: 161–169.

Karweil, J., 1969. Aktuell Probleme der Geochemie der Kohle. In: Advances in Organic Geochemistry 1968 (eds. P.A. Schenk and I. Havernaar): 59–84. Pergamon Press, Oxford.

Kędzior, A., Gradziński, R., Doktor, M., Gmur, D. 2007. Sedimentary history of a Mississippian to Pennsylvanian coal-bearing succession: an example from the Upper Silesia Coal Basin, Poland. Geological Magazine, **144**: 487–496.

Kotarba, M., 1988. Geochemical criteria for the origin of natural gases accumulated in the Upper Carboniferous coal-seam-bearing formation in Wałbrzych Coal Basin (in Polish with English summary). Stanisław Staszic University of Mining and Metallurgy Scientific Bulletin, 1199, Geology AGH, **42**: 1–119.

Kotarba, M., 1990a. Origin of gases accumulated in Upper Carboniferous coal-bearing strata of Lower Silesian Coal Basin and southern part of Rybnik Coal district (in Polish with English summary). In: Górotwór jako ośrodek wielofazowy. Wyrzuty skalno-gazowe (ed. J. Litwiniszyn): 37–49. Instytut Mechaniki Górotworu, Polska Akademia Nauk, Kraków.

Kotarba, M., 1990b. Origin of natural gases accumulated in the Upper Carboniferous formation in central field of "Thorez" coal mine: stable isotope studies (in Polish with English summary). In: Górotwór jako ośrodek wielofazowy. Wyrzuty skalno-gazowe. Instytut Mechaniki Górotworu (ed. J. Litwiniszyn): 51–65. Polska Akademia Nauk, Kraków.

Kotarba, M., 1990c. Isotopic geochemistry and habitat of the natural gases from Upper Carboniferous Žacleř coal-bearing formation in Nowa Ruda coal district (Lower Silesia, Poland). Organic Geochemistry, **16**: 549–560.

Kotarba, M.J., 2001. Composition and origin of coalbed gases in the Upper Silesian and Lublin Basins, Poland. Organic Geochemistry, **32**: 163–180.

Kotarba, M.J., Clayton, J.L., 2003. A stable isotope and biological marker study of Polish bituminous coals and carbonaceous shales. International Journal of Coal Geology, **55**: 73–94.

Kotarba, M.J., Lewan, M.D., 2004. Characterizing thermogenic coalbed gas from Polish coals of different ranks by hydrous pyrolysis. Organic Geochemistry, **35**: 615–646.

Kotarba, M.J., Lewan, M.D., 2013. Sources of natural gases in Middle Cambrian reservoirs in Polish and Lithuanian Baltic Basin as determined by stable isotopes and hydrous pyrolysis of Lower Palaeozoic source rocks. Chemical Geology, **345**: 62–76.

Kotarba, M.J., Pluta, I., 2009. Origin of natural waters and gases within the Upper Carboniferous coal-bearing and autochthonous Miocene strata in south-western part of the Upper Silesian Coal Basin, Poland. Applied Geochemistry, **24**: 876–889.

Kotarba, M.J., Rice, D.D., 2001. Composition and origin of coalbed gases in the Lower Silesian basin, northwestern Poland. Applied Geochemistry, **16**: 895–910.

Kotarba, M., Kosakowski, P., Botor, D., 1995a. Modelowanie metodą GENEX i bilans generowania węglowodorów w kompleksie skał iłowcowo-mułowcowych utworów produktywnych górnego karbonu Górnośląskiego Zagłębia Węglowego (in Polish). In: Opracowanie modeli oraz bilansu generowania i akumulacji gazów w serii węglonośnej Górnośląskiego Zagłębia Węglowego (eds. R. Ney and M. Kotarba): 115–130. Wydawnictwo Centrum PPGSMiE PAN, Kraków.

Kotarba, M., Ney, R., Hołda, S., 1995b. Bilans akumulacji metanu w pokładach węgla kamiennego i w kompleksie skał iłowcowo-mułowcowych górnego karbonu produktywnego Górnośląskiego Zagłębia Węglowego (in Polish). In: Opracowanie modeli oraz bilansu generowania i akumulacji gazów w serii węglonośnej Górnośląskiego Zagłębia Węglowego (eds. R. Ney

and M. Kotarba): 175–179. Wydawnictwo Centrum PPGSMiE PAN, Kraków.

Kotarba, M.J., Clayton, J.L., Rice, D.D., Wagner, M., 2002. Assessment of hydrocarbon source rock potential of Polish bituminous coals and carbonaceous shales. Chemical Geology, **184**: 11–35.

Kotarba, M.J., Curtis, J.B., Lewan, M.D., 2009. Comparison of natural gases accumulated in Oligocene strata with hydrous pyrolysis from Menilite Shales of the Polish Outer Carpathians. Organic Geochemistry, **40**: 769–783.

Kotarba, M.J., Nagao, K., Karnkowski P.H., 2014. Origin of gaseous hydrocarbons, noble gases, carbon dioxide and nitrogen in Carboniferous and Permian strata of the distal part of the Polish Basin: Geological and isotopic approach. Chemical Geology, **383**: 164–179.

Kotarba, M.J., Sumino, H., Nagao, K., 2019a. Origin of hydrocarbon and noble gases, carbon dioxide and molecular nitrogen in Devonian, Pennsylvanian and Miocene strata of the Polish Lublin and Ukrainian Lviv basins, southern part of the Upper Silesian Coal Basin and western part of the Carpathian Foredeep (Poland). Applied Geochemistry, **108**: 104371.

Kotarba, M.J., Więcław, D., Bilkiewicz, E., Radkovets, N.Y., Koltun, Y.V., Kmiecik, N., Romanowski, T., Kowalski, A., 2019b. Origin and migration of oil and natural gas in the western part of the Ukrainian Outer Carpathians: geochemical and geological approach. Marine and Petroleum Geology, **103**: 596–619.

Kotarba, M.J., Więcław, D., Bilkiewicz, E., Lillis, P.G., Dziadzio, P., Kmiecik, N., Romanowski, T., Kowalski, A., 2020a. Origin, migration and secondary processes of oil and natural gas in the central part of the Polish Outer Carpathians. Marine and Petroleum Geology, **121**: 104617.

Kotarba, M.J., Bilkiewicz, E., Więcław, D., Radkovets, N.Y., Koltun, Y.V., Kowalski, A., Kmiecik, N., Romanowski, T., 2020b. Origin and migration of oil and natural gas in the central part of the Ukrainian outer Carpathians: geochemical and geological approach. AAPG Bulletin, **104**: 1323–1356.

Kotarba, M.J., Bilkiewicz, E., Kosakowski, P., 2020c. Origin of hydrocarbon and non-hydrocarbon (H_2S, CO_2 and N_2) components of natural gas accumulated in the Zechstein Main Dolomite carbonate reservoir of the western part of the Polish sector of the Southern Permian Basin. Chemical Geology, **554**: 119807.

Kotas, A., 1982. Zarys budowy geologicznej Górnośląskiego Zagłębia Węglowego (in Polish). Przewodnik 54 Zjazdu Pol. Tow. Geol. Sosnowiec: 45–72. Wyd. Geol., Warszawa.

Kotas, A., (ed.), 1994. Coalbed methane potential of the Upper Silesian Coal Basin (Poland). Prace Państwowego Instytutu Geologicznego, **142**: 1–81.

Kotas, A., 1995. Upper Silesian Coal Basin – lithostratigraphy and sedimentologic-palegeographic development. Prace Państwowego Instytutu Geologicznego, **148**: 124–134.

Kotas, A., Porzycki, J., 1984. Geological position and main features of Carboniferous coal basins in Poland (in Polish with English summary). Przegląd Geologiczny, **32**: 268–280.

Kotas, A., Buła, Z., Gądek, S., Kwarciński, J., Malicki, R., 1983. Atlas geologiczny Górnośląskiego Zagłębia Węglowego, 1:100 000 (in Polish). Instytut Geologiczny, Warszawa.

Kowalski, A., Kotarba, M., Semyrka, G., 1995. Model i bilans generowania gazów z pokładów węgla utworów górnego karbonu Górnośląskiego Zagłębia Węglowego (in Polish). In: Opracowanie modeli oraz bilansu generowania i akumulacji gazów w serii węglonośnej Górnośląskiego Zagłębia Węglowego (eds. R. Ney and M. Kotarba): 99–114. Wydawnictwo Centrum PPGSMiE PAN, Kraków.

Kozłowska, A., Waksmundzka, M.I., 2020. Diagenesis, sequence stratigraphy and reservoir quality of the Carboniferous deposits of the south eastern Lublin Basin (SE Poland). Geological Quarterly, **64** (2): 422–459.

Kozłowska, A., Nurkiewicz, B., Różkowska, J., Cudak, J., 2015. Wyniki badań petrograficznych, mineralogicznych, geochemicznych i chemiczno-technologicznych (in Polish). Profile Głębokich Otworów Wiertniczych Państwowego Instytutu Geologicznego**, 144**: 106–177.

Krooss, B.M., Littke, R., Müller, B., Frielingsdorf, J., Schwochau, K., Idiz, E.F., 1995. Generation of nitrogen and methane from sedimentary organic matter: implications on the dynamics of natural gas accumulations. Chemical Geology, **126**: 291–318.

Krooss, B.M., Friberg, L., Gensterblum, Y., Hollenstein, J., Prinz, D., Littke, R., 2005. Investigation of the pyrolytic liberation of molecular nitrogen from Paleozoic sedimentary rocks. International Journal of Earth Sciences, **94**: 1023–1038.

Krooss, B.M., Plessen, B., Machel, H.G., Lüders, V., Littke, R., 2008. Origin and distribution of non-hydrocarbon gases. In: Dynamics of Complex Intracontinental Basins (eds. R. Littke, U. Bayer, D. Gajewski and S. Nelskamp): 433–458. Springer, Berlin-Heidelberg.

Kruszewska, K., 1983. Microfacies types of coal seams in Upper Silesian Coal Basin. Kwartalnik Geologiczny, **27** (1): 41–58.

Krzywiec, P., Mazur, S., Gągała, Ł., 2017. Late Carboniferous thin-skinned compressional deformation above the SW edge of the East European craton as revealed by seismic reflection and potential field data – correlations with the Variscides and the Appalachians. GSA Memoir, **213**: 353–372.

Kufrasa, M., Stypa, A., Krzywiec, P., Słonka, Ł., 2019. Late Carboniferous thin-skinned deformation in the Lublin Basin, SE Poland: results of combined seismic data interpretation, structural restoration and subsidence analysis. Annales Societatis Geologorum Poloniae, **89**: 175–194.

Landais, P., 1991. Assessment of coal potential evolution by experimental simulation of natural coalification. Organic Geochemistry, **17**: 705–710.

Lewan, M.D., 1985. Evaluation of petroleum generation by hydrous pyrolysis experimentation. Philosophical Transactions of the Royal Society, London, Ser. A., **315**: 123–134.

Lewan, M.D., 1993. Laboratory simulation of petroleum formation: Hydrous pyrolysis, In: Organic Geochemistry (eds. M. Engel and S. Macko). Plenum Publications Corp. New York: 419–442.

Lewan, M.D., 1997. Experiments on the role of water in petroleum formation. Geochimica et Cosmochimica Acta, **61**: 3691–3723.

Lewan, M.D., 2002. New insights on timing of oil and gas generation in the central Gulf Coast interior zone based on hydrous-pyrolysis kinetic parameters. Gulf Coast Association of Geological Societies, **52**: 607–620.

Lewan, M.D., Kotarba, M.J., 2014. Thermal-maturity limit for primary thermogenic-gas generation from humic coals as determined by hydrous pyrolysis. AAPG Bulletin, **98**: 2581–2610.

Littke, R., Krooss, B.M., Idiz, E.F., Frielingsdorf, J., 1995. Molecular nitrogen in natural gas accumulations: generation from sedimentary organic matter at high temperatures. AAPG Bulletin, **79**: 410–430.

Lu, S.T., Kaplan, I.R. 1990. Hydrocarbon-generating potential of humic coals from dry pyrolysis. AAPG Bulletin, **74**: 163–173.

Lüders, V., Reutel, Ch., Hoth, P., Banks, D.A., Mingram, B., Pettke, T., 2005. Fluid and gas migration in the North German Basin: fluid inclusion and stable isotope constrains. International Journal of Earth Sciences, **94**: 990–1009.

Lüders, V., Plessen, B., di Primio, R., 2012. Stable carbon isotopic ratios of CH_4–CO_2-bearing fluid inclusions in fracture-fill mineralization from the Lower Saxony Basin (Germany) – a tool for tracing gas sources and maturity. Marine and Petroleum Geology, **30**: 174–183.

Milkov, A.V., Etiope, G., 2018. Revised genetic diagrams for natural gases based on a global dataset of >20,000 samples. Organic Geochemistry, **125**: 109–120.

Mingram, B., Hoth, P., Lüders, V., Harlov, D., 2005. The significance of fixed ammonium in Palaeozoic sediments for the generation of nitrogen-rich natural gases in the North German Basin. International Journal of Earth Sciences, **94**: 1010–1022.

Misiak, J., 2017. Petrographic composition and forms of bituminous coal lithotypes in the Upper Carboniferous Formations of the Upper Silesian Coal Basin (in Polish with English summary). Gospodarka Surowcami Mineralnymi, **33**: 109–120.

Narkiewicz, M., 2007. Development and inversion of Devonian and Carboniferous basins in the eastern part of the Variscan foreland (Poland). Geological Quarterly, **51** (3): 231–256.

Narkiewicz, M., 2020. The Variscan foreland in Poland revisited: new data and new concepts. Geological Quarterly, **64** (2): 377–401.

Ni, Y., Liao, F., Gao, J., Chen, J., Yao, L., Zhang, D., 2019a. Hydrogen isotopes of hydrocarbon gases from different organic facies of the Zhongba gas field, Sichuan Basin, China. Journal of Petroleum Science and Engineering, **179**: 776–786.

Ni, Y., Liao, F., Yao, L., Gao, J., Zhang, D., 2019b. Hydrogen isotope of natural gas from the Xujiahe Formation and its implications for water salinization in central Sichuan Basin, China. Journal of Natural Gas Geoscience, **4**: 215–230.

Orr, W.L., 1977. Geologic and geochemical controls on the distribution of hydrogen sulphide in natural gas. In: Advances in Organic Geochemistry 1975 (eds. R. Campos and J. Goni): 571–597. Enadimsa, Madrid.

Oszczypko, N., Krzywiec, P., Popadyuk, I., Peryt, T., 2006. Carpathian Foredeep Basin (Poland and Ukraine): its sedimentary, structural, and geodynamic evolution. AAPG Memoir, **84**: 293–350.

Peryt, T.M., Buła, Z., Hałas, S., Olszewska, B., Pluta, I., Słodkowska, B., 2005. Non-marine evaporites in the Lower Miocene of Upper Silesia (Carpathian Foreland Basin, Poland). Geologica Carpathica, **56**: 327–336.

Porzycki, J., 1988a. Lithologic and sedimentologic characteristics of Carboniferous deposits (in Polish with English summary). Prace Państwowego Instytutu Geologicznego, **122**: 40–76, 229–231.

Porzycki, J., 1988b. Tectonics (in Polish with English summary). Prace Państwowego Instytutu Geologicznego, **122**: 154–160, 237–238.

Porzycki, J., Zdanowski, A., 1995a. Southeastern Poland (Lublin Carboniferous Basin). Prace Państwowego Instytutu Geologicznego, **148**: 102–109.

Porzycki, J., Zdanowski, A., 1995b. Coal deposits. Lublin Coal Basin. Prace Państwowego Instytutu Geologicznego, **148**: 159–164.

Ptak, B., Różkowska, A., 1995. Geochemical Atlas of Coal Deposits of Upper Silesian Coal Basin (in Polish with English summary). Państwowy Instytut Geologiczny, Warszawa.

Qin, K., Yang, Q., Gua, S., Lu, Q., Shu, W., 1994. Chemical structure and hydrocarbon formation of the Huanxian brown coal, China. Organic Geochemistry, **21**: 333–341.

Schimmelmann, A., Lewan, M.D., Winsch, R.P., 1999. D/H isotope ratios of kerogen, bitumen, oil, and water in hydrous pyrolysis of source rocks containing kerogen types I, II, IIS, and III. Geochimica et Cosmochimica Acta, **63**: 3751–3766.

Schimmelmann, A., Boudou, J.P., Lewan, M.D., Wintsch, R.P., 2001. Experimental controls on D/H and $^{13}C/^{12}C$ ratios of kerogen, bitumen and oil during hydrous pyrolysis. Organic Geochemistry, **32**: 1009–1018.

Sechman, H., Kotarba, M.J., Fiszer, J., Dzieniewicz, M., 2013. Distribution of methane and carbon dioxide concentrations in the near-surface zone and their genetic characterization at the abandoned "Nowa Ruda" coal mine (Lower Silesian Coal Basin, SW Poland). International Journal of Coal Geology, **116–117**: 1–16.

Sechman, H., Kotarba, M.J., Dzieniewicz, M., Romanowski, T., Fiszer, J., 2017. Evidence of methane and carbon dioxide migration to the near surface zone in the area of the abandoned coal mines in Wałbrzych District (Lower Silesian Coal Basin, SW Poland) based on periodical changes of molecular and isotopic compositions. International Journal of Coal Geology, **183**: 138–160.

Shuai, Y., Zhang, S., Peng, P., Zou, Y., Yuan, X., Liu, J., 2013. Occurrence of heavy carbon dioxide of organic origin: Evidence from confined dry pyrolysis of coal. Chemical Geology **358**: 54–60.

Smith, J.W., Gould, K.W., Rigby, D., 1982. The stable isotope geochemistry of Australian coals. Organic Geochemistry, **3**: 111–131.

Smith, J.W., Gould, K.W., Rigby, D., Hart, G., Hargraves, A.J., 1985. An isotopic study of hydrocarbon generation processes. Organic Geochemistry, **8**: 341–347.

Suleimenov, O.M., Krupp, R.E., 1994. Solubility of hydrogen sulfide in pure water and in NaCl solution, from 20 to 320°C and at saturation pressures. Geochimica et Cosmochimica Acta, **58**: 2433–2444.

Teerman, S.C., Hwang, R.J., 1991. Evaluation of the liquid hydrocarbon potential of coal by artificial maturation techniques. Organic Geochemistry, **6**: 749–764.

Tomaszczyk, M., Jarosiński, M., 2017. The Kock Fault Zone as an indicator of tectonic stress regime changes at the margin of the East European Craton (Poland). Geological Quarterly, **61** (4): 908–925.

Waksmundzka, M.I., 1998. Depositional architecture of the Carboniferous Lublin Basin (in Polish with English summary). Prace Państwowego Instytutu Geologicznego, **165**: 89–100.

Waksmundzka, M.I., 2010. Sequence stratigraphy of Carboniferous paralic deposits in the Lublin Basin (SE Poland). Acta Geologica Polonica, **60**: 557–597.

Waksmundzka, M.I., 2013. Carboniferous coarsening-up ward and non-gradational cyclothems in the Lublin Basin (SE Poland): palaeoclimatic implications. Geological Society Special Publications, **376**: 141–175.

Whiticar, M.J., 1994. Correlation of natural gases with their sources. AAPG Memoir, **60**: 261–283.

Więcław, D., Bilkiewicz, E., Kotarba, M.J., Lillis, P.G., Dziadzio, P.S., Kowalski, A., Kmiecik, N., Romanowski, T., Jurek, K., 2020. Origin and secondary processes in petroleum in the eastern part of the Polish Outer Carpathians. International Journal of Earth Sciences, **109**: 63–99.

Zdanowski, A., (ed.), 1999. Geological Atlas of the Lublin Coal Basin (in Polish with English summary). Państwowy Instytut Geologiczny, Warszawa.

Zdanowski, A., 2007. The Carboniferous of the Appalachian and its comparison to the Carboniferous of the Upper Silesian and Lublin Coal basins (in Polish with English summary). Geology AGH, **33**: 317–327.

Zhu, Y., Shi, B., Fang, C., 2000. The isotopic compositions of molecular nitrogen: implications on their origins in natural gas accumulations. Chemical Geology, **164**: 321–330.

Zielińska, M., Fabiańska, M., Więcław, D., Misz-Kennan, M., 2020. Comparative petrography and organic geochemistry of different types of organic matter occurring in the Outer Carpathians rocks. Geological Quaternary, **64** (1): 165–184.

Żaba, J., 1999. The structural evolution of Lower Palaeozoic succession in the Upper Silesia Block and Małopolska Block border zone (southern Poland) (in Polish with English summary). Prace Państwowego Instytutu Geologicznego, **166**: 1–162.